

Learning to generate new indoor scenes

Pulak Purkait
The University of Adelaide
pulak.isi@gmail.com

Christopher Zach
Chalmers University of Technology
christopher.m.zach@gmail.com

Ian Reid
The University of Adelaide
ian.reid@adelaide.edu.au

Abstract

Deep generative models have been used in recent years to learn coherent latent representations in order to synthesize high quality images. In this work we propose a neural network to learn a generative model for sampling consistent indoor scene layouts. Our method learns the co-occurrences, and appearance parameters such as shape and pose, for different objects categories through a grammar-based auto-encoder, resulting in a compact and accurate representation for scene layouts. In contrast to existing grammar-based methods with a user-specified grammar, we construct the grammar automatically by extracting a set of production rules on reasoning about object co-occurrences in training data. The extracted grammar is able to represent a scene by an augmented parse tree. The proposed auto-encoder encodes these parse trees to a latent code, and decodes the latent code to a parse tree, thereby ensuring the generated scene is always valid. We experimentally demonstrate that the proposed auto-encoder learns not only to generate valid scenes (i.e. the arrangements and appearances of objects), but it also learns coherent latent representations where nearby latent samples decode to similar scene outputs. The obtained generative model is applicable to several computer vision tasks such as 3D pose and layout estimation from RGB-D data.

1. Introduction

Recently proposed approaches for deep generative models have seen great success in producing high quality RGB images [6, 14, 15, 22] and continuous latent representations from images [10]. Our work aims to learn coherent latent representations for generating natural indoor scenes comprising different object categories and their respective appearances (pose and shape). Such a learned representation has direct use for various computer vision and scene understanding tasks, including (i) 3D scene-layout estimation [25], (ii) 3D visual grounding [3, 27], (iii) Visual Question Answering [1, 16], and (iv) robot navigation [18].

Developing generative models for such discrete domains

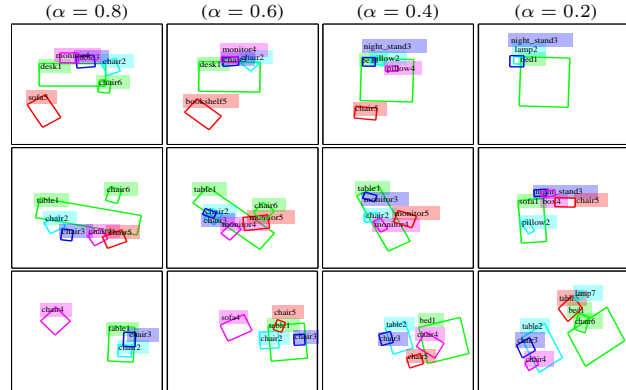


Figure 1. Synthetic scenes decoded from linear interpolations $\alpha\mu_1 + (1 - \alpha)\mu_2$ of the means μ_1 and μ_2 of the latent distributions of two very different scenes. Best viewed electronically.

has been explored in a limited number of works [8, 21, 30]. These works utilize prior knowledge of indoor scenes by manually defining attributed grammars. However, the number of rules in such grammars can be prohibitively large for real indoor environments, and consequently, these methods are evaluated only on synthetic data with a small number of objects. Further, the Monte Carlo based inference method can be intractably slow: up to 40 minutes [21] or one hour [8] to estimate a single layout.

Deep generative models for discrete domains have been proposed in [5] (employing sequential representations) and in [12] (based on formal grammars). In our work, we extend [12] by integrating object attributes, such as pose and shape of objects in a scene. Further, the underlying grammar is often defined manually [12, 21], but we propose to extract suitable grammar rules from training data automatically. The main components of our approach are thus:

- a scene grammar variational autoencoder (SG-VAE) that captures the appearances (pose and shape) of objects in the same 3D spatial configurations in a compact latent code (Section 2); the quality of the smooth latent code is illustrated by interpolating different scenes in Figure 1;
- a context free grammar that explains causal relationships among objects which frequently co-occur, automatically

- extracted from training data (Section 3);
- the practicality of the learned latent space is also demonstrated for a computer vision task.

Our SG-VAE is fast and has the ability to represent the scene in a coherent latent space as shown in Section 4.

2. Deep generative model for scene generation

The proposed method is influenced by the Grammar Variational Autoencoder [12], so we begin with a brief description of that prior art.

The Grammar VAE takes a valid string (in their case a chemical formula) and begins by parsing it into a set of production rules. These rules are represented as 1-hot binary vectors and encoded compactly to a latent code by the VAE. Latent codes can then be sampled and decoded to production rules and corresponding valid strings. More specifically, each production rule is represented by a 1-hot vector of size N , where N is the total number of rules, *i.e.* $N = |\mathcal{R}|$ (where \mathcal{R} is the set of rules). The maximum size T of the sequence is fixed in advance. Thus the scene is represented by a sequence $\mathcal{X} \in \{0, 1\}^{N \times T}$ of 1-hot vectors (note that when fewer than T rules are needed, a dummy/null rule is used to pad the sequence up to length T ensuring that the input to the autoencoder is always the same size). \mathcal{X} is then encoded to a continuous (low)-dimensional latent posterior distribution $\mathcal{N}(\mu(\mathcal{X}), \Sigma(\mathcal{X}))$. The decoding network, which is a recurrent network, maps latent vectors to a set of unnormalized log probability vectors (logits) corresponding to the production rules. To convert from the output logits to a valid sequence of production rules, each logit vector is considered in turn. The max output in the logit vector gives a 1-hot encoding of a production rule, but only some sequences of rules are valid. To avoid generating a rule that is inconsistent with the rules that have preceded it, invalid rules are masked out of the logit and the max is taken over only unmasked elements. This ensures that the Grammar VAE only ever generates valid outputs. Further details of the Grammar VAE can be found in [12].

Adapting this idea to the case of generating scenes requires that we incorporate not only valid co-occurrences of objects, but also valid attributes such as absolute pose (3D location and orientation) and shape (3D bounding boxes) of the objects in the scene. More specifically, our proposed SG-VAE is adapted from the Grammar VAE in the following ways:

- The object attributes, *i.e.* absolute pose (3D location and orientation) and shape (3D bounding boxes) of the objects are estimated while inferring the production rules.
- The SG-VAE is moreover designed to generate valid 3D scenes which adhere not only to the rules of grammar concerning co-occurrence, but also generate valid poses.

2.1. Scene-Grammar Variational Autoencoder

We represent the objects in indoor scenes explicitly by a set of production rules, so that the entire arrangement—*i.e.* the occurrences and appearances of the objects in a scene—is guaranteed to be consistent during inference. Nevertheless we also aim to capture the advantages of deep generative models in admitting a compact representation that can be rapidly decoded. While a standard VAE would implicitly *encourage* decoded outputs to be scene-like, our proposed solution extends the Grammar VAE [12] to explicitly enforce an underlying grammar, while still possessing the aforementioned advantages of deep generative models. For example, given an appearance of an object *bed*, the model finds strong evidence for co-occurrence of another indoor object, *e.g.* *dresser*. Furthermore, given the attributes (3D pose and bounding boxes) of one object (*bed*), the attributes of the latter (*dresser*) can be inferred.

The model comprises two parts: **(i)** a context free grammar (CFG) that represents valid configurations of objects; **(ii)** a Variational Autoencoder (VAE) that maps a sequence of production rules (*i.e.* a valid scene) to a low dimensional latent space, and decodes a latent vector to a sequence of production rules which in turn define a valid scene. We describe each of these two parts in the sub-sections below.

2.2. CFG of indoor scenes

A context-free grammar can be defined by a 4-tuple of sets $G = (S, \Sigma, \mathcal{V}, \mathcal{R})$ where S is a distinct non-terminal symbol known as start symbol; Σ is the finite set of non-terminal symbols; \mathcal{V} is the set of terminal symbols; and \mathcal{R} is the set of production rules. Note that in a CFG, the left hand side is always a non-terminal symbol. A set of all valid configurations \mathcal{C} derived from the production rules defined by the CFG G is called a language. In contrast to [21] where the grammar is pre-specified, we propose a data-driven algorithm to generate a set of production rules that constitutes a CFG.

We select a few objects and associate a number of non-terminals. Only those objects that lead to co-occurrence of other objects also exist as non-terminals (described in detail in Section 3.2). A valid production rule is thus “*an object category, corresponding to a non-terminal, generates another object category*”. For clarity, non-terminals are denoted in upper-case with the object name. For example *BED* and *bed* are the non-terminal and the terminal symbols corresponding to the object category *bed*. Thus occurrence of a non-terminal *BED* leads to occurrence of the immediate terminal symbol *bed* and possibly further occurrences of other terminal symbols that *bed* co-occurs with, *e.g.* *dresser*. Thus, a set of rules $\{S \rightarrow \text{scene SCENE}; \text{SCENE} \rightarrow \text{bed BED SCENE}; \text{BED} \rightarrow \text{bed BED}; \text{BED} \rightarrow \text{dresser BED}; \text{BED} \rightarrow \text{None}; \text{SCENE} \rightarrow \text{None}\}$ can be defined accordingly. Note that an additional object category *scene*

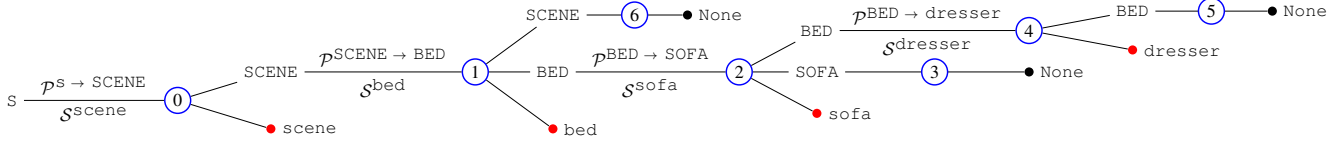


Figure 2. An example of parse tree obtained by applying the CFG to a scene comprising bed, sofa, dresser. The sequence of production rules ①-⑥ are marked in order. The pose and shape attributes of production rules are displayed above and below of the rules. Note that attributes corresponding to None are zero and not shown above.

is incorporated to represent the shape and size of the room. The learned scene grammar is composed of following rules:

- (R1) *involving start symbol S*: generates the terminal `scene` and non-terminal `SCENE` that represents the indoor scene layout with attributes as the room size and room orientation, *e.g.* $S \rightarrow \text{scene} \text{ SCENE};$. This rule ensures generating a room first.
- (R2) *involving nonterminal SCENE*: generates a terminal and a non-terminal corresponding to an object category, *e.g.* $\text{SCENE} \rightarrow \text{bed} \text{ BED} \text{ SCENE};$.
- (R3) *generating a terminal object category*: a non-terminal generates a terminal corresponding to another object category, *e.g.* $\text{BED} \rightarrow \text{dresser} \text{ BED};$.
- (R4) *involving None*: a non-terminal symbol is assigned to `None`, *e.g.* $\text{BED} \rightarrow \text{None};$.

`None` is an empty object and corresponding rule is a dummy rule indicating that the generation of the nonterminal is complete and the parser is now ready to handle the next non-terminal in the stack. The proposed method to deduce a CFG from data is described in detail in Section 3.

2.3. The VAE network

Let \mathcal{D} be a set of scenes comprising multiple objects. Let \mathcal{S}_i^j be the (bounding box) shape parameters and $\mathcal{P}_i^j = (T_i^j; \gamma_i^j)$ be the (absolute) pose parameters of j th object in the i th scene where T_i^j is the center and γ_i^j is the (yaw) angle corresponding to the direction of the object in the horizontal plane, respectively. Note that an object bounding box is aligned with gravity, thus there is only one degree of freedom in its orientation. The world co-ordinates are aligned with the camera co-ordinate frame.

The pose and shape attributes $\Theta^{j \rightarrow k} = (\mathcal{P}_i^{j \rightarrow k}, \mathcal{S}_i^k)$ are associated with a production rule in which a non-terminal X_j yields a terminal X_k . The pose parameters $\mathcal{P}_i^{j \rightarrow k}$ of the terminal object X_k are computed w.r.t. the non-terminal object X_j on the left of the production rule. *i.e.* $\mathcal{P}_i^{j \rightarrow k} = (\mathcal{P}_i^{j-1})^{-1} \mathcal{P}_i^k$. The absolute poses of the objects are determined by chaining the relative poses on the path from the root node to the terminal node in the parse tree (see Figure 2). Note that pose and shape attributes of the production rules corresponding to `None` object are fixed to zero.

The VAE must encode and decode both production rules (1-hot vectors) and the corresponding pose and shape

parameters. We achieve this by having separate initial branches of the encoder into which the attributes $\Theta^{j \rightarrow k}$, and the 1-hot vectors are passed. Features from the 1-hot encoding branch and the pose-shape branch are then concatenated after a number of 1D convolutional layers. These concatenated features undergo further 1D convolutional layers before being flattened and mapped to the latent space (thereby predicting μ and Σ of $\mathcal{N}(\mu, \Sigma)$). The decoding network is a recurrent network consisting of a stack of GRUs, that takes samples $z \sim \mathcal{N}(\mu, \Sigma)$ (employing reparameterization trick [10]) and outputs logits (corresponding to the production rules) and corresponding attributes $\Theta^{j \rightarrow k}$. Logits corresponding to invalid production rules are masked out.

The reconstruction loss of our SG-VAE consists of two parts: (i) a cross entropy loss corresponding to the 1-hot encoding of the production rules—note that *soft-max* is computed only on the components after mask-out—and (ii) a mean squared error loss corresponding to the production rule attributes (but omitting the terms of `None` objects). Thus, the loss is given as follows:

$$\mathcal{L}_{total}(\phi, \theta; \mathcal{X}, \Theta) = \mathcal{L}_{vae}(\phi, \theta; \mathcal{X}) + \lambda_1 (\mathcal{L}_{pose}(\phi, \theta; \mathcal{P}) + \lambda_2 \mathcal{L}_{shape}(\phi, \theta; \mathcal{S})) \quad (1)$$

where \mathcal{L}_{vae} is the autoencoder loss [12], and \mathcal{L}_{pose} and \mathcal{L}_{shape} are mean squared error loss corresponding to pose and shape parameters, respectively; ϕ , and θ are the encoder and decoder parameters of the autoencoder that we optimize; (\mathcal{X}, Θ) are the set of training examples comprising 1-hot encoders and rule attributes. Instead of directly regressing the orientation parameter, the respective *sines* and *cosines* are regressed. Our choice is $\lambda_1 = 10$ and $\lambda_2 = 1$ in all experiments.

3. Discovery of the scene grammar

In much previous work a grammar is manually specified. However in this work we aim to discover a suitable grammar for scene layouts in a data-driven manner. In this section we describe our method. It comprises two parts. First we generate a causal graph of all pairwise relationships discovered in the training data, as described in more detail in Section 3.1. Second we prune this causal graph by removing all but the dominant discovered relationships, as

described in Section 3.2.

3.1. Data-driven relationship discovery

We aim to discover causal relationships of different objects that reflects the influence of the appearance of one object to another. We learn the relationship using hypothesis testing, with each successful hypothesis added to a causal graph (directed) $\mathcal{G} : (\mathcal{V}, \mathcal{E})$ where the vertex set $\mathcal{V} = \{X_1, \dots, X_n\}$ is the set of different object categories, and edge set \mathcal{E} is the set of causal relationships. An edge $(X_j \rightarrow X_{j'}) \in \mathcal{E}$ corresponds to a direct causal influence on occurrence of the object X_j to the object $X_{j'}$. We conduct separate **(i)** appearance based and **(ii)** co-occurrence based testing for causal relationships between a pair of object categories as set out below.

(i) Testing for dependency based on co-occurrences We seek to capture loose associations (*e.g.* sofa and TV) and determine if these associations have a potentially causal nature. To do so, for each pair of object categories we then consider whether these categories are dependent, given a third category. This is performed using the Chi-squared (χ^2) test described below. If the dependence persists across all possible choices of the third category, we conclude that the dependence is not induced by another object, therefore a potentially causal link should exist between them. This exhaustive series of tests is $O(Nm^3)$, where N is the number of scenes and m is the number of categories (in our case, 84). However it is performed offline and only once. This procedure creates an undirected graph with links between pairs where a causal relationship is hypothesized to exist. To establish the direction of causation—*i.e.* turn the undirected graph into a directed one, we use Pearl’s Inductive Causation algorithm [19] and the procedure is summarized in Algorithm 2 of the appendix.

In more detail the χ^2 -test checks for conditional independence of a pair of object categories $\{X_j, X_{j'}\}$ given an additional object category $X_k \in \mathcal{V} \setminus \{X_j, X_{j'}\}$. The probabilities required for the test are obtained from the relative frequencies of the objects and their co-occurrences in the dataset. Algorithm 1 describes this in detail. By way of example, *pillow* and *blanket* might co-occur in a substantial number of scenes, however, their co-occurrences are influenced by a third object category *bed*. In this case, the pairwise relationship between *pillow* and *blanket* is determined to be independent, given the presence of *bed*, so no link between *pillow* and *blanket* is created.

(ii) Testing for dependency based on shape and pose In addition to the conditional co-occurrence relationships captured above, we also seek to capture covering/enclosing and supporting relationships—which are defined by the shape and pose of the objects as well as the categories—in the

Algorithm 1: χ^2 -test for cond independence check

Input: Co-occurrences O of the objects $X_j, X_{j'}, X_k$

Output: **True** if $X_j \perp\!\!\!\perp X_{j'} \mid X_k$ and **False** Otherwise

```

1  $\chi^2 = \sum_{j, j', k \in \{0, 1\}} (O_{j, j', k} - O_{j, k}O_{j', k}/O_k)^2 / (O_{j, k}O_{j', k}/O_k),$ 
    $O_{j, j', k}$ : frequency of occurrences of  $(j, j', k)$ ,
    $O_{j, k}$  : frequency of occurrences of  $(j, k)$ ,
    $O_k$  : frequency of occurrences of  $k$ ,  $N$  : number of scenes
2 Compute  $p$ -value from cumulative  $\chi^2$  distribution with
   above  $\chi^2$  value and d.o.f. ; /* D.o.f is 2 */
3 return  $p$ -value  $< \tau$  (we choose  $\tau = 0.05$ )

```

causal graph. More precisely we hypothesize a causal relationship between object categories A and B if:

- object category A is found to support object category B (*i.e.* their relative poses and shapes are such that, within a threshold, one is above and touching the other), or,
- object category B is enclosed/covered by another larger object category A (again this is determined using a threshold on the objects’ relative shapes and poses).

We accept a hypothesis and establish the causal relationship (by entering a suitable edge into the causal graph) if at least 30% of the co-occurrences of these object categories in the dataset agree with the hypothesis. The final directed causal relational graph \mathcal{G} is the union of the causal graphs generated by the above tests. Note that we do not consider any dependencies that would lead to a cycle in the graph [4]. The result of the procedure is also displayed in Figure 3.

3.2. Creating a CFG from the causal graph

We now need to create a Context Free Grammar from the causal graph. The CFG is characterised by non-terminal symbols that generate other symbols. Suppose we choose a particular node in the causal graph (*i.e.* an object category) and assume it is non-terminal. By tracing the full set of directed edges in the causal graph emanating from this node we create a set of production rules. This non-terminal and associated rules are then tested against the dataset to determine how many scenes are explained (formally “covered”) by the rules. A good choice of non-terminals will lead to good coverage. Our task then is to determine an optimal set of non-terminals and associated rules to give the best coverage of the full dataset of scenes.

Note that finding such a set is a combinatorial hard problem. Therefore, we devise a greedy algorithm to select non-terminals and find approximate best coverage. Let X_j , an object category, be a potential non-terminal symbol and \mathcal{R}_j be the set of production rules derived from X_j in the causal graph. Let C_j be the set of terminals that \mathcal{R}_j covers (essentially nodes that X_j leads to in \mathcal{G}). Our greedy algorithm begins with an empty set $\mathcal{R} = \emptyset$ and chooses the node X_j and

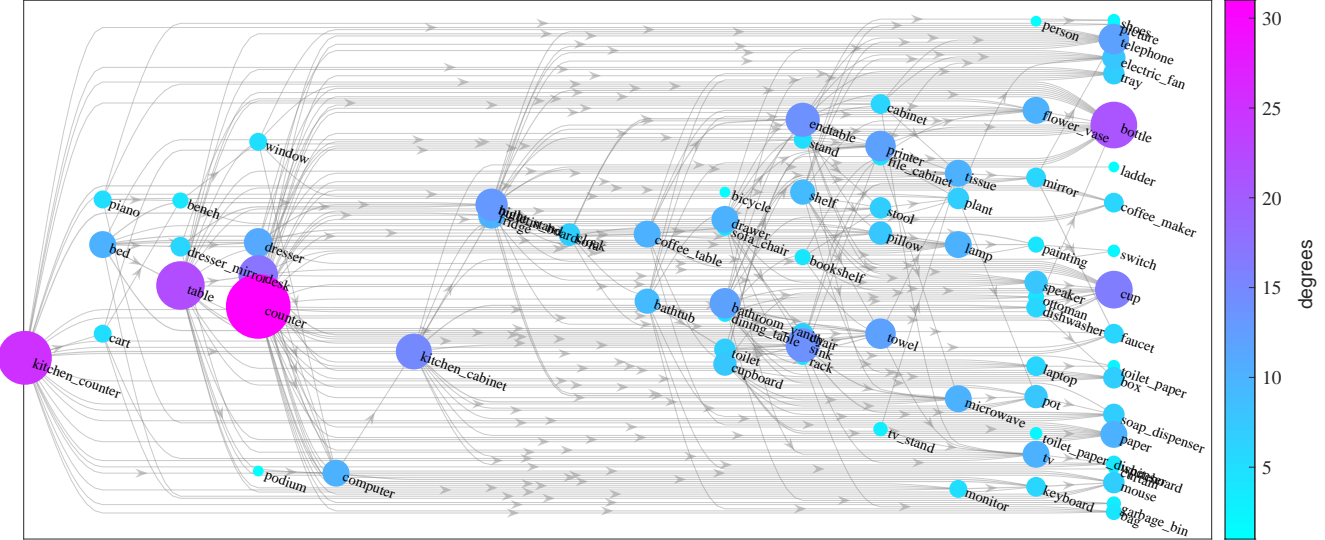


Figure 3. The above graph is generated by the modified IC algorithm on SUNRGBD-3D Dataset. An arrowhead of an edge indicates the direction of causation and the color of a node indicates its degree.

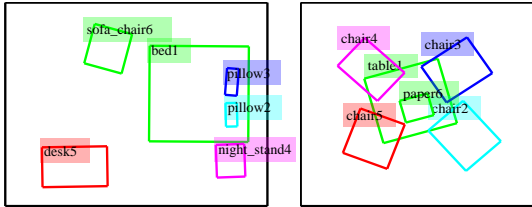


Figure 4. The parsing order is displayed by a numeral concatenated with the object name. Left: the objects are sorted in the order of precedence defined by the grammar, and Right: multiple chairs are sorted in the appearance w.r.t. the table in anti-clockwise direction.

associated production rule set \mathcal{R}_j to add that maximize the *gain* in coverage $\mathcal{G}_{gain}(\mathcal{R}_j, \mathcal{R}) = \frac{1}{|\mathcal{R}_j|} \sum_{I_i \in \mathcal{I} \setminus \mathcal{C}} |Y_i| / |I_i|$.

Unique parsing Given a scene there could be multiple parse trees derived by the leftmost derivation grammar and hence produces different sequences and different representations. For example, for a scene consist of `bed`, `sofa` and `pillow`, the terminal object `pillow` could be generated by any of the non-terminals `BED` or `SOFA`. This ambiguity can confuse the parser while encoding a scene. Further, different orderings of multiple occurrences of an object lead to different parse trees. We consider following parsing rules to remove the ambiguity:

- Fix the order of the object categories in the order of precedence defined by the grammar.
- Multiple occurrences of an object are sorted in the appearance w.r.t. the preceded object in the anti-clockwise direction. One such example is shown in Figure 4.

Note that this ordering is only required during training.

4. Experiments

Dataset We evaluate the proposed method on SUN RGB-D Dataset [24] consisting of 10,335 real scenes with 64,595 3D bounding boxes and about 800 object categories. The dataset is a collection of multiple datasets [9, 23, 28], and is highly unbalanced: *e.g.* a single object category `chair` corresponds to about 31% of all the bounding boxes and 38% of total object categories occur just once in the entire dataset. We consider object categories appearing at least 10 times in the dataset for evaluation. Further, very similar object categories are merged, yielding 84 object categories and 62,485 bounding boxes. We separated 10% of the data at random for validation. On average there are 4.29 objects per image and maximum number of objects in an image is considered to be 15. This also provides the upper bound of the length of the sequence generated by the grammar. Note that the dataset is the intersection of the given dataset and the scene language, *i.e.* the possible set of scenes that can be generated by the CFG.

Baseline methods for evaluation

- (BL1) *Variant of SG-VAE*: In contrast to the proposed SG-VAE where attributes of each rule are directly concatenated with 1-hot encoding of the rule, in this variant separate attributes for each rule type are predicted by the decoder and rest are filled with zeros.
- (BL2) *No Grammar VAE* [5]: No grammar is considered in this baseline. The 1-hot encodings correspond to the object type is concatenated with the absolute pose of the objects (in contrast to rule-type and relative pose in SG-VAE) respectively.
- (BL3) *Grammar VAE* [12] + *Make home* [30]: The Gram-

Table 1. Results of 3D object reconstructions of some of the frequent objects in the dataset under a valid reconstruction with $\text{IoU} > 0.25$. The pose estimation results are furnished within braces where the angular errors are shown in degrees and displacement errors are in meters.

	chair	bed	table	sofa	ktchn.cntr	piano
SG-VAE	92.38 (5.88°, 0.13m)	100.0 (2.80°, 0.08m)	96.29 (2.84°, 0.08m)	84.45 (5.65°, 0.10m)	100.0 (1.69°, 0.08m)	67.1 (6.93°, 0.11m)
BL1	75.44 (8.30°, 0.14m)	98.51 (5.70°, 0.09m)	93.88 (3.70°, 0.08m)	82.56 (6.94°, 0.15m)	100.0 (1.62°, 0.06m)	48.7 (10.3°, 0.12m)
BL2 [5]	33.77 (28.1°, 0.32m)	75.14 (7.12°, 0.45m)	90.26 (7.69°, 0.33m)	0.00 (—, —)	83.29 (5.96°, 0.09m)	0.80 (45.1°, 0.43m)
BL3 [12]+[30]	29.22 (41.8°, 0.26m)	88.72 (35.7°, 0.58m)	72.95 (56.7°, 0.34m)	60.95 (47.2°, 0.67m)	100.0 (52.5°, 0.78m)	26.3 (17.4°, 0.33m)

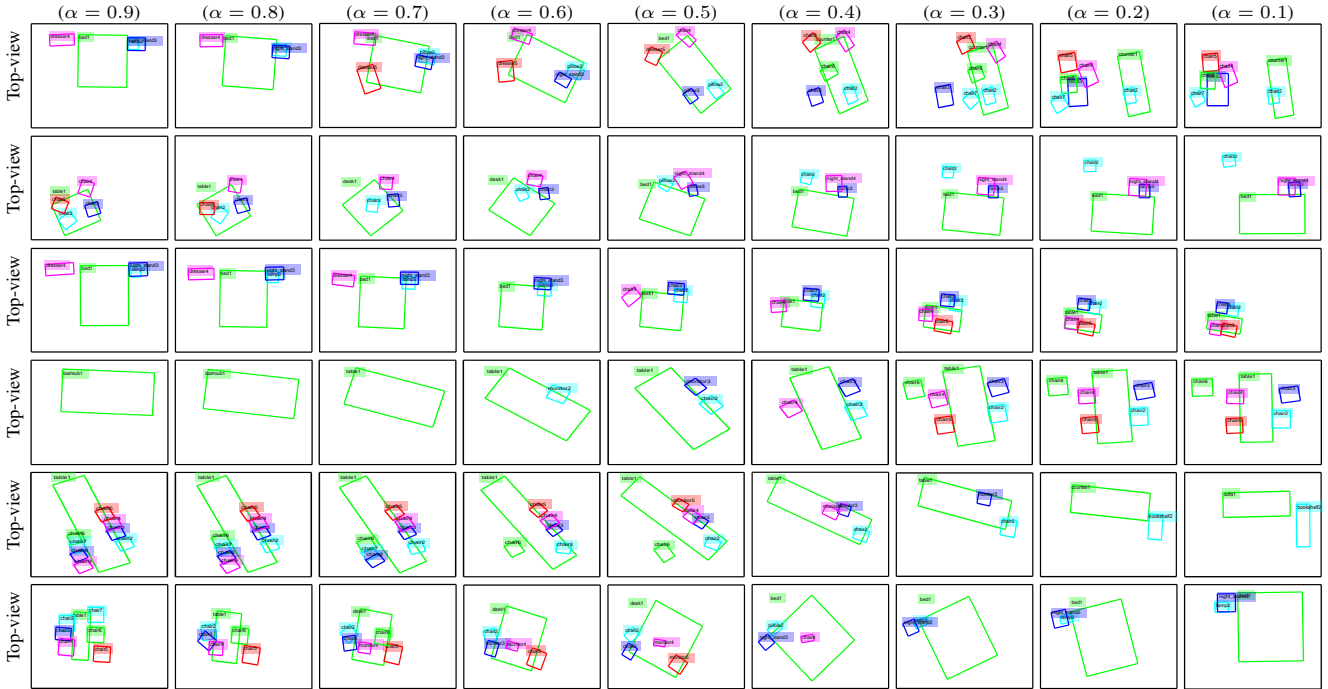


Figure 5. Synthetic scenes decoded from linear interpolations $\alpha\mu_1 + (1 - \alpha)\mu_2$ of the means μ_1 and μ_2 of the latent distributions of two separate scenes. The generated scenes are valid in terms of the co-occurrences of the object categories and their shapes and poses (more examples can be found in the appendix). The room-size and the camera view-point are fixed for better visualization. Best viewed electronically.

Table 2. IoU of room layout estimation

Methods	SG-VAE	BL1	BL2 [5]	BL3 [12]+[30]
Grammar	✓	✓		✓
Pose & Shape	✓	✓	✓	

IoU	0.6240	0.5673	0.2964	0.5119
-----	--------	--------	--------	--------

mar VAE is incorporated with our extracted grammar to sample a set of coherent objects and [30] is used to arrange them. Sampled 10 times and solution corresponding to best IoU w.r.t. groundtruth is employed. The details of the above baselines are provided in the appendix.

All the baselines including SG-VAE are implemented in python 2.7 (Tensorflow) and trained on a GTX 1080 Ti GPU. The relevant source codes are shared ¹ for reproducibility.

Evaluation metrics The relative poses of individual objects in a scene are accumulated to compute their absolute poses which are then combined with the shape parameters to compute the scene layout. The reconstructed scene layouts are then compared against the groundtruth layouts.

- **3D Object reconstruction** We employed IoU to measure the shape similarity of the bounding boxes. Reconstructed bounding boxes with $\text{IoU} > 0.25$ are considered as true positives. The results are reported in Table 1.
- **3D Pose estimation** The average pose error is considered over two separate metrics: (i) angular error in degrees, (ii) displacement error in meters (see Table 1).
- **Room Layout Estimation** The evaluation is conducted as the IoU of the *occupied* space between the groundtruth and the predicted layouts (see Table 2). The intersection is computed only over the true positives.

Interpolation in latent space Two distinct scenes are encoded into the latent space, *e.g.*, $\mathcal{N}(\mu_1, \Sigma_1)$ and

¹<https://github.com/pulak09/SG-VAE>

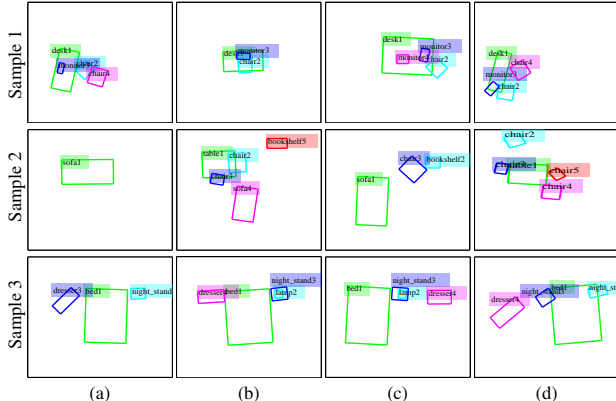


Figure 6. Arithmetic in latent space: latent vector of (d) is obtained by the sum of latent vectors of (a) & (b) and subtracted by (c), *i.e.* (d) := (a) + (b) - (c). Note that in all the cases the synthesized scenes in (d) are meaningful in terms of arithmetic operations.

$\mathcal{N}(\mu_2, \Sigma_2)$ and new scenes are then synthesized from regular linear interpolated vectors of the means, *i.e.* from $\alpha\mu_1 + (1-\alpha)\mu_2$. We performed the experiment on a set of random pairs chosen from the test dataset. The results are displayed in Figure 11. Notice that the proposed SG-VAE always yields a valid and realistic scene.

Arithmetic in latent space We attempt to manipulate scenes by conducting arithmetic operations on the latent vectors. The latent codes of two scenes are added and subtracted by the third. A new scene is synthesized from the resultant latent code. We observe that in most cases, the resultant latent vector captures the inherent concept of manipulation over the objects. Some examples are shown in Figure 13 where the manipulated latent vectors produce synthesized scene adhere to the arithmetic operations. We also observe manipulation in pose and shape of objects in the scenes, *e.g.* in Sample 1, two horizontal larger desks canceled each other and we see a thinner tilted desk in the output. A similar behavior can be observed for sofa in Sample 2 and bed in Sample 3.

4.1. Comparison with baselines on other datasets

The conventional indoor scene synthesis methods (for example, GRAINS [14], Human-centric [21] (HC), fast-synth [22](FS) etc.) are tailored to and trained on SUNCG dataset [26]. The dataset consists of synthetic scenes generated by graphic designers. Moreover, the dataset is no longer publicly available (along with the meta-files). Therefore the following evaluation protocols are employed to assess the performance of different methods.

Qualitative comparison To conduct a qualitative evaluation, we employ a classifier (based on Pointnet [20]) to predict a scene layout to be an original or generated by a

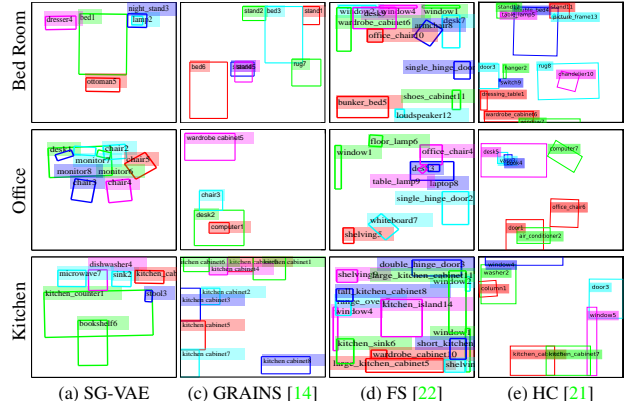


Figure 7. Top-views of the synthesized scenes generated by the proposed and the baseline indoor scene synthesis methods.

Table 3. Original vs. synthetic classification accuracy for the scenes generated by different methods. The accuracy indicates that the synthetic scenes are indistinguishable from the original scenes and hence lower (closer to 50%) is better.

Methods	Pointnet [20]			Visual Inspection		
	SG-VAE	GRAINS [14]	HC [21]	SG-VAE	GRAINS [14]	HC [21]
Accuracy	71.3%	96.4%	98.1%	63.2%	82.9%	87.4%

scene synthesis method. If the generated scenes are very similar to the original scenes, the classifier performs poorly (lower accuracy) and indicates the efficacy of the synthesis method. The classifier takes a scene layout of multiple objects, individually represented by the concatenation of 1-hot code and the attributes, as input and predicts a binary label according to the scene-type. The classifier is trained and tested on a dataset of $2K$ original and synthetic scenes (50% training and 50% testing). Note that SG-VAE is trained on the synthetic data generated by the interpolations of latent vectors (some examples are shown in Figure 11) and real data of SUN RGB-D [24]. Lower accuracy of the classifier validates the superior performance of the proposed SG-VAE. The same task is performed by 10 human subjects on 10% scenes of the dataset. The average performance is plotted in Table 3. Examples of some synthetic scenes generated by other baselines² are also shown in Figure 7.

Runtime comparison All the methods are evaluated on a single CPU and the runtime is displayed in Table 4. Note that the decoder of the proposed SG-VAE takes only ~ 1 ms to generate the parse tree and the rest of the time is consumed by the renderer (generating bounding boxes). The proposed method is almost two orders of magnitude faster than the other scene synthesis methods.

²We thank the authors of GRAINS [14] and HC [21] for sharing the code and the authors of FS [22] for the results displayed in Figure 7.



Figure 8. A few results on SUNRGBD Dataset inferred from the RGB-D images. Best viewed electronically.

Table 4. Average time required to generate a single scene.

Methods	SG-VAE	GRAINS [14]	FS [22]	HC [21]
Avg. runtime	8.5ms	$1.2 \times 10^2 ms$	$1.8 \times 10^3 ms$	$2.4 \times 10^5 ms$

4.2. Scene layout estimation from the RGB-D image

The task is to predict the 3D scene layout given an RGB-D image. Typically, the state of the art methods are based on sophisticated region proposals and subsequent processing [25]. With this experiment, we aim to demonstrate the potential use of the latent representation learned by the proposed auto-encoder for a computer vision task, and therefore we employ a simple approach at this point. We (linearly) map deep features (extracted from images by a DNN [33]) to the latent space of the scene-grammar autoencoder. The decoder subsequently generates a 3D scene configuration with associated bounding boxes and object labels from the projected latent vector. Since during the deep feature extraction and the linear projection, the spatial infor-

Table 5. IoU for RGBD to room layout estimation

Methods	SG-VAE	BL1	BL2 [5]	BL3 [12]+[30]	DSS [25]
IoU	0.4387	0.4315	0.4056	0.4259	0.4070

mation of the bounding boxes are lost, the predicted scene layout is then combined with a bounding box detection to produce the final output.

The bounding box detector of DSS [25] is employed and the scores of the detection are updated based on our reconstruction as follows: the score (confidence of the prediction) of a detected bounding box is doubled if a similar bounding box (in terms of shape and pose) of the same category is reconstructed by our method. A 3D non-maximum suppression is applied to the modified scores to get the final scene layout. The details can be found in the appendix.

We selected the average IoU for room layout estimation as the evaluation metric, and the results are presented in Table 5. The proposed method and other grammar-based baselines improve (in terms of average IoU) the scene lay-

out estimation from the same by sophisticated methods such as deep sliding shapes [25]. Furthermore, the proposed method tackles the problem in a much simpler and faster way. Thus, it can be employed to any 3D scene layout estimation method with very little overhead (*e.g.* a few ms in addition to 5.6s of [25]). Results on some test images where SG-VAE produces better IoUs are displayed in Figure 8.

5. Related Works

The most relevant method to ours is GRAINS [14]. It requires training separate networks for each of the room-types—bedroom, office, kitchen etc. HC [21] is very slow and takes a few minutes to synthesize a single layout. FS [22] is fast, but still takes a couple of seconds. Scene-GraphNet [29] predicts a probability distribution over object types that fits well in a target location given an incomplete layout. Further, all these methods are tailored to and trained on the synthetic SUNCG dataset and therefore can not be applied to any real-world applications.

Koppula *et al.* [11] propose a graphical model that captures the local visual appearance and co-occurrences of different objects in the scene. They learn the appearance relationships among objects from the visual features that takes an RGB-D image as input and predicts 3D semantic labels of the objects as output. The pair-wise support relationships of the indoor objects are also exploited in [7, 23].

Grammar-based models for 3D scene reconstruction have been partially exploited before [31, 32], *e.g.* textured probabilistic grammar [13]. Zhao *et al.* [31] proposed hand-coded grammar to its terminal symbols (line segments) and later extended to different functional groups in [32]. Choi *et al.* [2] proposed a 3D geometric phrase model that estimates a scene layout with multiple object interactions. Note that all the above methods are based on hand-coded production rules, in contrast, the proposed method exploits a self-supervision to yield the production rules of the grammar.

6. Conclusion

We proposed a grammar-based autoencoder SG-VAE for generating natural indoor scene layouts containing multiple objects. By construction the output of SG-VAE always yields a valid configuration (w.r.t. the grammar) of objects, which was also experimentally confirmed. We demonstrated that the obtained latent representation of an SG-VAE has desirable properties such as the ability to interpolate between latent states in a meaningful way. The latent space of SG-VAE can also be easily adapted to computer vision problems (*e.g.* 3D scene layout estimation from RGB-D images). Nevertheless, we believe that there is potential in leveraging the latent space of SG-VAEs to the other tasks, *e.g.* fine-tuning the latent space for a consistent layout over multiple cameras which is part of the future work.

References

- [1] Peter Anderson, Xiaodong He, Chris Buehler, Damien Teney, Mark Johnson, Stephen Gould, and Lei Zhang. Bottom-up and top-down attention for image captioning and visual question answering. In *Proceedings of CVPR*, pages 6077–6086, 2018. 1
- [2] Wongun Choi, Yu-Wei Chao, Caroline Pantofaru, and Silvio Savarese. Understanding indoor scenes using 3d geometric phrases. In *Proceedings of CVPR*, pages 33–40, 2013. 9
- [3] Chaorui Deng, Qi Wu, Qingyao Wu, Fuyuan Hu, Fan Lyu, and Mingkui Tan. Visual grounding via accumulated attention. In *Proceedings of CVPR*, pages 7746–7755, 2018. 1
- [4] Dorit Dor and Michael Tarsi. A simple algorithm to construct a consistent extension of a partially oriented graph. 1992. 4, 14
- [5] Rafael Gómez-Bombarelli, Jennifer N Wei, David Duvenaud, José Miguel Hernández-Lobato, Benjamín Sánchez-Lengeling, Dennis Sheberla, Jorge Aguilera-Iparraguirre, Timothy D Hirzel, Ryan P Adams, and Alán Aspuru-Guzik. Automatic chemical design using a data-driven continuous representation of molecules. *ACS central science*, 4(2):268–276, 2018. 1, 5, 6, 8, 13
- [6] Ian Goodfellow, Jean Pouget-Abadie, Mehdi Mirza, Bing Xu, David Warde-Farley, Sherjil Ozair, Aaron Courville, and Yoshua Bengio. Generative adversarial nets. In *Proceedings of NIPS*, pages 2672–2680, 2014. 1
- [7] Ruiqi Guo and Derek Hoiem. Support surface prediction in indoor scenes. In *Proceedings of ICCV*, pages 2144–2151, 2013. 9
- [8] Siyuan Huang, Siyuan Qi, Yixin Zhu, Yinxue Xiao, Yuanlu Xu, and Song-Chun Zhu. Holistic 3d scene parsing and reconstruction from a single rgb image. In *Proceedings of ECCV*, pages 187–203, 2018. 1
- [9] Allison Janoch, Sergey Karayev, Yangqing Jia, Jonathan T Barron, Mario Fritz, Kate Saenko, and Trevor Darrell. A category-level 3d object dataset: Putting the kinect to work. In *Consumer depth cameras for computer vision*, pages 141–165. Springer, 2013. 5
- [10] Diederik P Kingma and Max Welling. Auto-encoding variational bayes. In *Proceedings of ICLR*, pages 469–477, 2014. 1, 3
- [11] Hema S Koppula, Abhishek Anand, Thorsten Joachims, and Ashutosh Saxena. Semantic labeling of 3d point clouds for indoor scenes. In *Proceedings of NIPS*, pages 244–252, 2011. 9
- [12] Matt J Kusner, Brooks Paige, and José Miguel Hernández-Lobato. Grammar variational autoencoder. In *Proceedings of ICML*, pages 1945–1954. JMLR. org, 2017. 1, 2, 3, 5, 6, 8, 13
- [13] Dan Li, Disheng Hu, Yuke Sun, and Yingsong Hu. 3d scene reconstruction using a texture probabilistic grammar. *Multimedia Tools and Applications*, 77(21):28417–28440, 2018. 9
- [14] Manyi Li, Akshay Gadi Patil, Kai Xu, Siddhartha Chaudhuri, Owais Khan, Ariel Shamir, Changhe Tu, Baoquan Chen, Daniel Cohen-Or, and Hao Zhang. Grains: Generative re-

cursive autoencoders for indoor scenes. *ACM Transactions on Graphics (TOG)*, 38(2):12, 2019. 1, 7, 8, 9

[15] Ming-Yu Liu and Oncel Tuzel. Coupled generative adversarial networks. In *Proceedings of NIPS*, pages 469–477, 2016. 1

[16] Jiasen Lu, Jianwei Yang, Dhruv Batra, and Devi Parikh. Hierarchical question-image co-attention for visual question answering. In *Proceedings of NIPS*, pages 289–297, 2016. 1

[17] Laurens van der Maaten and Geoffrey Hinton. Visualizing data using t-sne. *Journal of machine learning research*, 9(Nov):2579–2605, 2008. 11

[18] Jean-Arcady Meyer and David Filliat. Map-based navigation in mobile robots:: II. a review of map-learning and path-planning strategies. *Cognitive Systems Research*, 4(4):283–317, 2003. 1

[19] Judea Pearl and Thomas S Verma. A theory of inferred causation. In *Studies in Logic and the Foundations of Mathematics*, volume 134, pages 789–811. Elsevier, 1995. 4, 14

[20] Charles R Qi, Hao Su, Kaichun Mo, and Leonidas J Guibas. Pointnet: Deep learning on point sets for 3d classification and segmentation. In *Proceedings of CVPR*, pages 652–660, 2017. 7

[21] Siyuan Qi, Yixin Zhu, Siyuan Huang, Chenfanfu Jiang, and Song-Chun Zhu. Human-centric indoor scene synthesis using stochastic grammar. In *Proceedings of CVPR*, pages 5899–5908, 2018. 1, 2, 7, 8, 9

[22] Daniel Ritchie, Kai Wang, and Yu-an Lin. Fast and flexible indoor scene synthesis via deep convolutional generative models. In *Proceedings of CVPR*, pages 6182–6190, 2019. 1, 7, 8, 9

[23] Nathan Silberman, Derek Hoiem, Pushmeet Kohli, and Rob Fergus. Indoor segmentation and support inference from rgbd images. In *Proceedings of ECCV*, pages 746–760. Springer, 2012. 5, 9

[24] Shuran Song, Samuel P Lichtenberg, and Jianxiong Xiao. Sun rgbd: A rgbd scene understanding benchmark suite. In *Proceedings of CVPR*, pages 567–576, 2015. 5, 7, 11

[25] Shuran Song and Jianxiong Xiao. Deep sliding shapes for amodal 3d object detection in rgbd images. In *Proceedings of CVPR*, pages 808–816, 2016. 1, 8, 9, 12

[26] Shuran Song, Fisher Yu, Andy Zeng, Angel X Chang, Manolis Savva, and Thomas Funkhouser. Semantic scene completion from a single depth image. In *Proceedings of CVPR*, pages 1746–1754, 2017. 7

[27] Fanyi Xiao, Leonid Sigal, and Yong Jae Lee. Weakly-supervised visual grounding of phrases with linguistic structures. In *Proceedings of CVPR*, pages 5945–5954, 2017. 1

[28] Jianxiong Xiao, Andrew Owens, and Antonio Torralba. Sun3d: A database of big spaces reconstructed using sfm and object labels. In *Proceedings of ICCV*, pages 1625–1632, 2013. 5

[29] Evangelos Kalogerakis, Yang Zhou, Zachary White. Scene-graphnet: Neural message passing for 3d indoor scene augmentation. In *Proceedings of ICCV*, 2019. 9

[30] Lap-Fai Yu, Sai-Kit Yeung, Chi-Keung Tang, Demetri Terzopoulos, Tony F Chan, and Stanley J Osher. Make it home: automatic optimization of furniture arrangement. In *ACM Transactions on Graphics (TOG)*, volume 30, page 86. ACM, 2011. 1, 5, 6, 8, 13

[31] Yibiao Zhao and Song-Chun Zhu. Image parsing with stochastic scene grammar. In *Proceedings of NIPS*, pages 73–81, 2011. 9

[32] Yibiao Zhao and Song-Chun Zhu. Scene parsing by integrating function, geometry and appearance models. In *Proceedings of CVPR*, pages 3119–3126, 2013. 9

[33] Bolei Zhou, Agata Lapedriza, Jianxiong Xiao, Antonio Torralba, and Aude Oliva. Learning deep features for scene recognition using places database. In *Proceedings of NIPS*, pages 487–495, 2014. 8, 11, 12

Appendices

A. Selection of the CFG—Algorithm details

We aim to find suitable non-terminals and associated production rules that cover the entire dataset. Note that finding such a set is a combinatorial hard problem. Therefore, we devise a greedy algorithm to select non-terminals and find approximate best coverage. Let X_j , an object category, be a potential non-terminal symbol and \mathcal{R}_j be the set of production rules derived from X_j in the causal graph. Let C_j be the set of terminals that \mathcal{R}_j covers (essentially nodes that X_j leads to in the causal graph \mathcal{G}). Our greedy algorithm begins with an empty set $\mathcal{R} = \emptyset$ and chooses the node X_j and associated production rule set \mathcal{R}_j to add that maximize the *gain* in coverage

$$\mathcal{G}_{gain}(\mathcal{R}_j, \mathcal{R}) = \frac{1}{|\mathcal{R}_j|} \sum_{I_i \in \mathcal{I} \setminus \mathcal{C}} |Y_i| / |I_i| \quad (2)$$

where \mathcal{C} is the set of scenes that are already covered with a predefined fraction p by the set of rules \mathcal{R} , *i.e.* $\mathcal{C} = \{I_i \mid \frac{|Y_i|}{|I_i|} > p\}$ where Y_i is the set of terminal symbols occurs while parsing a scene I_i by \mathcal{R} . The algorithm continues till no further nodes and associated rule set contribute a positive gain or until the current rule set covers the entire dataset with probability p (chosen as 0.8). We name our algorithm as *p-cover* and is furnished in algorithm 3. Note that only object co-occurrences were utilized and object appearances were not incorporated in the proposed *p-cover* algorithm.

To ensure the production rules to form a CFG, we select a few vertices (anchor nodes) of the causal graph and associate a number of non-terminals. A valid production rule is “*an object category corresponding to an anchor node generates another object category it is adjacent to in \mathcal{G}* ”. Let us consider the set of anchor nodes forms our set of non-terminals Σ . The set of all possible objects including dummy *None* is defined as the set of terminal symbols \mathcal{V} .

Let \mathcal{R}_j be the set of production rules derived from a non-terminal X_j corresponding to an anchor object X_j , and C_j be the set of terminals that \mathcal{R}_j covers (essentially nodes that X_j leads to in \mathcal{G}). Note that \mathcal{R}_j contains mainly four types of production rules as described in [(R1)-(R4)] in the main text. A few examples of such set of production rules are displayed in Figure 10. The above strategy could lead to a large amount of production rules (ideally sum of number of the anchor points and the number of edges $|\mathcal{E}|$ in the causal graph). Note that a large number of production rules increases the problem complexity. Contrarily, an arbitrary selection of few rules leads to a small number of derivable scenes (language of constituent grammar). We propose an algorithm to find a compressed (minimal size) set of rules to

cover the entire dataset. Our underlying assumption is that the distribution of objects in the test scenes is very similar to the distribution of the same in the training scenes. Hence, we use the coverage of the training scenes as a proxy for the coverage of testing scenes and derive a probabilistic covering algorithm on the occurrences of objects in the dataset.

An example snippet for the grammar produced using this algorithm on the SUNRGBD dataset [24] is as follows:

$S \rightarrow \text{scene SCENE}$ $\text{SCENE} \rightarrow \text{bed BED SCENE}$ $\text{BED} \rightarrow \text{bed BED}$ $\text{BED} \rightarrow \text{lamp BED}$ $\text{Bed} \rightarrow \text{sofa SOFA BED}$ $\text{BED} \rightarrow \text{pillow PILLOW BED}$ $\text{BED} \rightarrow \text{night_stand BED}$ $\text{BED} \rightarrow \text{dresser BED}$ \dots $\text{BED} \rightarrow \text{None}$	$\text{SCENE} \rightarrow \text{sofa sofainc SCENE}$ $\text{SOFA} \rightarrow \text{sofa SOFA}$ $\text{SOFA} \rightarrow \text{pillow PILLOW SOFA}$ $\text{SOFA} \rightarrow \text{TOWEL SOFA}$ $\text{SOFA} \rightarrow \text{None}$ \dots $\text{SCENE} \rightarrow \text{None}$
---	--

The entire grammar is displayed in Section D. In the above snippet the non-terminal **BED** generates another non-terminal **SOFA** that leads to an additional set of production rules corresponding to **SOFA**. Note that the grammar is right-recursive and not a regular grammar as some of the rules contain two non-terminals in the right hand side.

Note that in this grammar non-terminal symbol **BED** generates another non-terminal **SOFA** which further leads to another set of production rules corresponding to **SOFA**. The grammar is right-recursive and not a regular grammar as some of the rules contain two non-terminals in the right hand side.

B. Visualization of the latent space

To check the continuity of the latent space, the latent vectors (*i.e.*, the mean μ of the distribution $\mathcal{N}(\mu, \Sigma)$) is projected to 2D plane using data visualization algorithm t-SNE [17]. In Figure 9, we display 15 different scenes in the latent space after t-SNE projection. We observe top left and top right regions are kitchen and bathroom scenes respectively. Whereas, top and bottom regions correspond to bedroom and dining room scenes respectively. The middle region mostly corresponds to living room and office scenes. Note that proposed SG-VAE not only considers the object co-occurrences, also considers object attributes (3D pose and shape parameters). For example, two scenes consists of a *chair* and a *table* are mapped to two nearby but distinct points.

C. Additional experiments

C.1. Scene layout from the RGB-D image—in detail

The task is to predict the 3D scene layout given an RGB-D image. We (linearly) map deep features (extracted from images by a DNN [33]) to the latent space of the scene-grammar autoencoder. The decoder subsequently

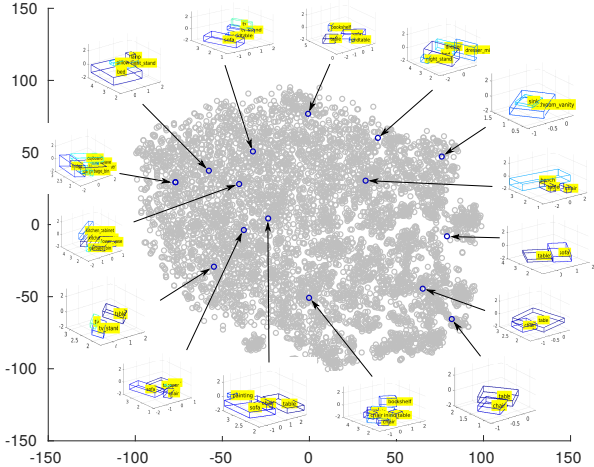


Figure 9. We plot the 2D projection of the mean μ of the encoded distributions of the data (encoded with 50 dimension) projected using t-SNE algorithm. 15 chosen scenes are also displayed. Note that points with similar semantic concepts are clustered around a certain region.

generates a 3D scene configuration with associated bounding boxes and object labels from the projected latent vector. Since during the deep feature extraction and the linear projection, the spatial information of the bounding boxes are lost, the predicted scene layout is then combined with a bounding box detection to produce the final output.

Training Let \mathcal{F}_i be the (in our case 8192-dimensional) deep feature vector extracted from the image I_i , and let $\mathcal{N}(\mu_i, \Sigma_i)$ be the (e.g. 50-dimensional) latent representation obtained by encoding the corresponding parse tree. We align the feature vector \mathcal{F}_i with the latent distribution using a linear mapping $\psi(\mathcal{F}_i) = A\mathcal{F}_i$, where A is a matrix to be learned from a training set $\mathcal{T} := \{I_i := (\mathcal{F}_i, \mu_i, \Sigma_i)\}$. We minimize the cross-entropy between the predicted (deterministic) latent representation $\psi(\mathcal{F}_i)$ and the target distribution $\mathcal{N}(\mu_i, \Sigma_i)$, therefore the optimal matrix A is determined as $\hat{A} = \arg \min_A \sum_{I_i \in \mathcal{T}} (A\mathcal{F}_i - \mu_i)^T \Sigma_i^{-1} (A\mathcal{F}_i - \mu_i) + \lambda \|A\|_2^2$. The features \mathcal{F}_i of dimension 8192 are then projected into the mean of the encoded vector μ_i (typically dimension 50). Let $\phi : \mathcal{F}_i \rightarrow \mu_i$ be the mapping that project the feature vectors \mathcal{F}_i to the latent space μ_i . A neural network could be used to learn the mapping ϕ , however, a simple linear projection is employed here, *i.e.* $\psi(\mathcal{F}_i) = A\mathcal{F}_i$. The mapping ϕ is learned from the training examples $Tr = \{I_i := (\mathcal{F}_i, \mu_i, \Sigma_i)\}$ as follows:

$$\hat{A} = \arg \min_A \sum_{I_i \in \mathcal{T}} \left(A\mathcal{F}_i - \mu_i \right)^T \Sigma_i^{-1} \left(A\mathcal{F}_i - \mu_i \right) + \lambda \|A\|_2^2 \quad (3)$$

where we also added a regularization term with weight λ

(chosen as $\lambda = 100$). Differentiating the objective to zero, we get $\sum_{I_i \in \mathcal{T}} \Sigma_i^{-1} \hat{A} (\mathcal{F}_i \mathcal{F}_i^T) + 2\lambda \hat{A} = \sum_{I_i \in \mathcal{T}} \Sigma_i^{-1} \mu_i \mathcal{F}_i^T$. Therefore,

$$\hat{A} = \left(\sum_{I_i \in Tr} \mathcal{F}_i^T \Sigma_i^{-1} \mathcal{F}_i + 2\lambda I \right)^{-1} \sum_{I_i \in Tr} \mathcal{F}_i \Sigma_i^{-1} \mu_i \quad (4)$$

Note that the covariance matrix Σ_i is chosen to be diagonal, and thus \hat{A} can be solved efficiently. The above is a system of linear equations solved by vectorizing the matrix \hat{A} .

Testing For test data image features [33] are extracted and then mapped to the latent space using the trained mapping $\hat{\phi}(\mathcal{F}_i) := \mathcal{F}_i \hat{A}$. The scenes are then decoded from the latent vectors $\hat{\mu} := \mathcal{F}_i \hat{A}$ using the decoder part of the SG-VAE. The bounding box detector of DSS [25] is employed and the scores of the detection are updated based on our reconstruction as follows: the score (confidence of the prediction) of a detected bounding box is doubled if a similar bounding box (in terms of shape and pose) of the same category is reconstructed by our method. A 3D non-maximum suppression is applied to the modified scores to get the final scene layout. Results on some test images where SG-VAE produces better IoUs are displayed in Figure 8.

C.2. Quality assessment of the autoencoder

The scenes and the bounding boxes of the test examples are first encoded to the latent representations $\mathcal{N}(\mu_i, \Sigma_i)$. The mean of the distributions μ_i are then decoded to the scene with object bounding boxes and labels. The results are displayed below. Ideally, the decoder should produce a scene which is very similar to input test scene. IoU (computed over the occupied space) of the decoded scene and the original input scene is also shown in the main paper. Baseline methods for evaluation as follows:

(BL1) Variant of SG-VAE: In contrast to the proposed SG-VAE where attributes of each rule are directly concatenated with 1-hot encoding of the rule, in this variant separate attributes for each rule type are predicted by the decoder and rest are filled with zeros. *i.e.*, the 1-hot encoding of the production rules is same as SG-VAE but the attributes are represented by a $|\mathcal{R}| * \theta$ dimensional vector where $|\mathcal{R}|$ is the number of production rules and θ is the size of the attributes. For example, the pose and shape attributes $\Theta^{j \rightarrow k} = (\mathcal{P}_i^{j \rightarrow k}, \mathcal{S}_i^{k})$, associated with a production rule (say p th rule) in which a non-terminal X_j yields a terminal X_k , are placed in $(p-1)*\theta + 1 : p*\theta$ dimensions of the attribute vector and rest of the positions are kept as zeros. Note that in case of SG-VAE the attributes are represented by a θ dimensional vector only.

(BL2) No Grammar VAE [5]: No grammar is considered in this baseline. The 1-hot encodings correspond to the object type is concatenated with the absolute pose of the objects (in contrast to rule-type and relative pose in SG-VAE) respectively. *i.e.* each object is represented by $|\mathcal{V}|$ dimensional 1-hot vector and a θ dimensional attribute vector. The objects are ordered in the same way as SG-VAE to avoid ambiguity in the representation. The same network as SG-VAE is incorporated except no grammar is employed (*i.e.* no masking) while decoding a latent vector to a scene layout.

(BL3) Grammar VAE [12] + Make home [30]: The Grammar VAE is incorporated with our extracted grammar to sample a set of coherent objects and [30] is used to arrange them. Sampled 10 times and solution corresponding to best IoU w.r.t. groundtruth is employed. Here no pose and shape attributes are incorporated while training the autoencoder. The attributes are estimated by *Make home* [30] and the best (in terms of IoU) is chosen comparing the ground-truth.

The results are shown in Figure 14. Note that in all the examples shown, *No Grammar VAE*, *i.e.* BL2 can not reconstruct the input scene whereas the SG-VAE performs the best. The detailed quantitative numbers are presented in the main manuscript.

D. Production rules of the CFG

The total number of rules generated by the algorithm described in section 3 of the main draft is 399, number of non-terminals is 49 and number of terminal objects is 84. In the following we display the entire learned grammar. Note again that the non-terminal symbols are displayed in upper case, S is the start symbol and *None* is the empty object. The rules are separated by semicolons ‘ ; ’ symbol.

```

S → scene SCENE;
SCENE → counter COUNTER SCENE;
COUNTER → chair CHAIR COUNTER;
COUNTER → cabinet CABINET COUNTER;
COUNTER → computer COMPUTER COUNTER;
COUNTER → monitor MONITOR COUNTER;
COUNTER → sink SINK COUNTER;
COUNTER → drawer DRAWER COUNTER;
COUNTER → keyboard KEYBOARD COUNTER;
COUNTER → ottoman OTTOMAN COUNTER;
COUNTER → fridge FRIDGE COUNTER;
COUNTER → printer PRINTER COUNTER;
COUNTER → microwave MICROWAVE COUNTER;
COUNTER → mirror MIRROR COUNTER;
COUNTER → speaker SPEAKER COUNTER;
COUNTER → clock CLOCK COUNTER;
COUNTER → box COUNTER;
COUNTER → garbage_bin COUNTER;
COUNTER → lamp COUNTER;
COUNTER → stool COUNTER;
COUNTER → paper COUNTER;
COUNTER → tv COUNTER;
COUNTER → bottle COUNTER;
COUNTER → laptop COUNTER;
COUNTER → towel COUNTER;
COUNTER → bag COUNTER;
COUNTER → cup COUNTER;
COUNTER → tray COUNTER;
COUNTER → mouse COUNTER;

```

```

COUNTER → telephone COUNTER;
COUNTER → pot COUNTER;
COUNTER → flower_vase COUNTER;
COUNTER → coffee_maker COUNTER;
COUNTER → dishwasher COUNTER;
COUNTER → None;
SCENE → KITCHEN_COUNTER KITCHEN_COUNTER SCENE;
KITCHEN_COUNTER → cabinet CABINET KITCHEN_COUNTER;
KITCHEN_COUNTER → monitor MONITOR KITCHEN_COUNTER;
KITCHEN_COUNTER → sink SINK KITCHEN_COUNTER;
KITCHEN_COUNTER → kitchen_cabinet KITCHEN_CABINET
KITCHEN_COUNTER;
KITCHEN_COUNTER → whiteboard WHITEBOARD
KITCHEN_COUNTER;
KITCHEN_COUNTER → fridge FRIDGE KITCHEN_COUNTER;
KITCHEN_COUNTER → plant PLANT KITCHEN_COUNTER;
KITCHEN_COUNTER → microwave MICROWAVE KITCHEN_COUNTER;
KITCHEN_COUNTER → cart CART KITCHEN_COUNTER;
KITCHEN_COUNTER → box KITCHEN_COUNTER;
KITCHEN_COUNTER → garbage_bin KITCHEN_COUNTER;
KITCHEN_COUNTER → stool KITCHEN_COUNTER;
KITCHEN_COUNTER → paper KITCHEN_COUNTER;
KITCHEN_COUNTER → tv KITCHEN_COUNTER;
KITCHEN_COUNTER → bottle KITCHEN_COUNTER;
KITCHEN_COUNTER → towel KITCHEN_COUNTER;
KITCHEN_COUNTER → bag KITCHEN_COUNTER;
KITCHEN_COUNTER → cup KITCHEN_COUNTER;
KITCHEN_COUNTER → tray KITCHEN_COUNTER;
KITCHEN_COUNTER → telephone KITCHEN_COUNTER;
KITCHEN_COUNTER → pot KITCHEN_COUNTER;
KITCHEN_COUNTER → soap_dispenser KITCHEN_COUNTER;
KITCHEN_COUNTER → coffee_maker KITCHEN_COUNTER;
KITCHEN_COUNTER → dishwasher KITCHEN_COUNTER;
KITCHEN_COUNTER → faucet KITCHEN_COUNTER;
KITCHEN_COUNTER → None;
SCENE → bed BED SCENE;
BED → chair CHAIR BED;
BED → table TABLE BED;
BED → pillow PILLOW BED;
BED → sofa SOFA BED;
BED → computer COMPUTER BED;
BED → night_stand NIGHT_STAND BED;
BED → dresser DRESSER BED;
BED → ottoman OTTOMAN BED;
BED → bench BENCH BED;
BED → dresser_mirror dresser_MIRROR BED;
BED → clock CLOCK BED;
BED → window WINDOW BED;
BED → lamp BED;
BED → mouse BED;
BED → stand BED;
BED → None;
SCENE → desk DESK SCENE;
DESK → chair CHAIR DESK;
DESK → computer COMPUTER DESK;
DESK → monitor MONITOR DESK;
DESK → drawer DRAWER DESK;
DESK → keyboard KEYBOARD DESK;
DESK → printer PRINTER DESK;
DESK → speaker SPEAKER DESK;
DESK → bulletin_board BULLETIN_BOARD DESK;
DESK → lamp DESK;
DESK → paper DESK;
DESK → bottle DESK;
DESK → laptop DESK;
DESK → cup DESK;
DESK → mouse DESK;
DESK → telephone DESK;
DESK → switch DESK;
DESK → flower_vase DESK;
DESK → tissue DESK;
DESK → shoes DESK;
DESK → stand DESK;
DESK → None;
SCENE → bathroom_vanity BATHROOM_VANITY SCENE;
BATHROOM_VANITY → sink SINK BATHROOM_VANITY;
BATHROOM_VANITY → curtain CURTAIN BATHROOM_VANITY;
BATHROOM_VANITY → mirror MIRROR BATHROOM_VANITY;
BATHROOM_VANITY → box BATHROOM_VANITY;
BATHROOM_VANITY → bottle BATHROOM_VANITY;
BATHROOM_VANITY → towel BATHROOM_VANITY;
BATHROOM_VANITY → cup BATHROOM_VANITY;
BATHROOM_VANITY → tray BATHROOM_VANITY;
BATHROOM_VANITY → tissue BATHROOM_VANITY;
BATHROOM_VANITY → soap_dispenser BATHROOM_VANITY;
BATHROOM_VANITY → coffee_maker BATHROOM_VANITY;
BATHROOM_VANITY → faucet BATHROOM_VANITY;
BATHROOM_VANITY → None;
SCENE → bathtub BATHTUB SCENE;
BATHTUB → toilet TOILET BATHTUB;
BATHTUB → curtain CURTAIN BATHTUB;
BATHTUB → stool BATHTUB;
BATHTUB → door BATHTUB;
BATHTUB → bottle BATHTUB;
BATHTUB → towel BATHTUB;
BATHTUB → bag BATHTUB;
BATHTUB → cup BATHTUB;
BATHTUB → tray BATHTUB;
BATHTUB → flower_vase BATHTUB;
BATHTUB → soap_dispenser BATHTUB;
BATHTUB → None;
SCENE → cupboard CUPBOARD SCENE;
CUPBOARD → sink SINK CUPBOARD;
CUPBOARD → file_cabinet FILE_CABINET CUPBOARD;
CUPBOARD → printer PRINTER CUPBOARD;

```

Algorithm 2: Unsupervised structure learning: Modified Inductive Causation (IC) [19]

Input: a dataset \mathcal{D} of natural scenes formed by a set of objects $\mathcal{V} = \{X_1, \dots, X_n\}$

Output: a graph $\mathcal{G} = (\mathcal{V}, \mathcal{E})$ representing the causal relationships between the variables

```

1 Initialize  $\mathcal{G} := \{\mathcal{V}; \mathcal{E} = \mathcal{E}_0\}$ ; /* Initialize graph with prior edges */
2 for every pair of objects  $(X_j \in \mathcal{V}; X_{j'} \in \mathcal{V})$  do
3   for every conditioning variable  $X_k \in \mathcal{V} \setminus \{X_i, X_{j'}\}$  do
4     hypothesis test  $X_j \perp\!\!\!\perp X_{j'} \mid X_k \text{ in } \mathcal{D}$ ; /* Using Conditional Algo 1 */
5     if no independence was found then
6       add an undirected edge  $(X_j, X_{j'})$  in  $\mathcal{E}$ , i.e.,  $\mathcal{E} = \mathcal{E} \cup (X_j, X_{j'})$ .
7   for every pair of objects  $(X_j \in \mathcal{V}; X_{j'} \in \mathcal{V})$  with a common neighbor  $X_k$  do
8     if  $(X_j, X_{j'}) \notin \mathcal{E}$  then
9       if one of  $(X_k, X_j)$  and  $(X_k, X_{j'})$  is directed and the other is undirected or
10      both are undirected then
11        turn the triplet into a common parent structure, i.e.,  $X_j \leftarrow\!\!\!\leftarrow X_k \rightarrow\!\!\!\rightarrow X_{j'}$ 
12 Propagate the arrow orientation for all undirected edges (modify the set  $\mathcal{E}$  accordingly) without introducing a
13 directed cycle. ; /* Following Dor and Tarsi [4] */
14 return  $\mathcal{G} = \{\mathcal{V}, \mathcal{E}\}$ 

```

Algorithm 3: p-Cover : A greedy algorithm for p-covering the dataset

Input: a dataset \mathcal{D} of indoor scenes \mathcal{I} formed by a set of objects $\mathcal{V} = \{X_1, \dots, X_n\}$, the causal graph $\mathcal{G} = (\mathcal{V}, \mathcal{E})$ obtained by Algorithm 2 and a probability p (chosen as 0.8)

Output: a set of rules \mathcal{R} that explains the occurrences of objects in the scenes \mathcal{I}

```

1 Choose the set of potential non-terminals as  $\mathcal{V}' = \{X_i \in \mathcal{V} : \text{deg}_{\text{out}}(X_i)/(\text{deg}_{\text{in}}(X_i) + \epsilon) > 1\}$ ;
2 Generate set of concepts and associated rules  $\{\mathcal{R}_j\}_{j \in \mathcal{V}'}$  by choosing adjacent objects; /* Some examples
   are displayed in Figure 10 */
3 Initialize  $\mathcal{R} \leftarrow \emptyset$ ,  $\mathcal{V}^* \leftarrow \emptyset$ , and  $C = \emptyset$ ; /* Initialize by an empty set; */
4 while the cover set  $C$  covers the dataset with probability  $p$  do
5   for every non-terminal and associated set of rules  $\mathcal{R}_j, \forall j \in \mathcal{V}' \setminus \mathcal{V}^*$  do
6     | Compute the gain  $\mathcal{G}_{\text{gain}}(\mathcal{R}_j, \mathcal{R})$  as referred in Eq. 2 of the main draft
7     | compute next anchor node  $X_j = \arg \max_{X_j \in \mathcal{V}' \setminus \mathcal{V}^*} \mathcal{G}_{\text{gain}}(\mathcal{R}_j, \mathcal{R})$  and  $\mathcal{V}^* = \mathcal{V}^* \cup X_j$ 
8     |  $\mathcal{R} = \mathcal{R} \cup \mathcal{R}_j$ 
9     |  $C = C \cup C_j$ ; /* Update the rule set and the cover set; */
10 |  $\mathcal{R} = \mathcal{R} \cup [S \rightarrow \text{'None'}]$ 
11 return  $\mathcal{R}$ 

```

CUPBOARD → air-conditioner AIR-CONDITIONER CUPBOARD;	TABLE → lamp TABLE;
CUPBOARD → box CUPBOARD;	TABLE → stool TABLE;
CUPBOARD → cup CUPBOARD;	TABLE → paper TABLE;
CUPBOARD → pot CUPBOARD;	TABLE → bottle TABLE;
CUPBOARD → soap_dispenser CUPBOARD;	TABLE → laptop TABLE;
CUPBOARD → None;	TABLE → towel TABLE;
SCENE → kitchen_cabinet KITCHEN_CABINET SCENE;	TABLE → cup TABLE;
KITCHEN_CABINET → sink SINK KITCHEN_CABINET;	TABLE → tray TABLE;
KITCHEN_CABINET → fridge FRIDGE KITCHEN_CABINET;	TABLE → mouse TABLE;
KITCHEN_CABINET → microwave MICROWAVE KITCHEN_CABINET;	TABLE → telephone TABLE;
KITCHEN_CABINET → lamp KITCHEN_CABINET;	TABLE → pot TABLE;
KITCHEN_CABINET → paper KITCHEN_CABINET;	TABLE → flower_vase TABLE;
KITCHEN_CABINET → bottle KITCHEN_CABINET;	TABLE → tissue TABLE;
KITCHEN_CABINET → bag KITCHEN_CABINET;	TABLE → coffee_maker TABLE;
KITCHEN_CABINET → switch KITCHEN_CABINET;	TABLE → None;
KITCHEN_CABINET → soap_dispenser KITCHEN_CABINET;	SCENE → shelf SHELF SCENE;
KITCHEN_CABINET → coffee_maker KITCHEN_CABINET;	SHELF → computer COMPUTER SHELF;
KITCHEN_CABINET → dishwasher KITCHEN_CABINET;	SHELF → plant PLANT SHELF;
KITCHEN_CABINET → faucet KITCHEN_CABINET;	SHELF → microwave MICROWAVE SHELF;
KITCHEN_CABINET → None;	SHELF → speaker SPEAKER SHELF;
SCENE → table TABLE SCENE;	SHELF → box SHELF;
TABLE → chair CHAIR TABLE;	SHELF → picture SHELF;
TABLE → computer COMPUTER TABLE;	SHELF → bottle SHELF;
TABLE → monitor MONITOR TABLE;	SHELF → towel SHELF;
TABLE → keyboard KEYBOARD TABLE;	SHELF → cup SHELF;
TABLE → printer PRINTER TABLE;	SHELF → telephone SHELF;
TABLE → speaker SPEAKER TABLE;	SHELF → electric_fan SHELF;

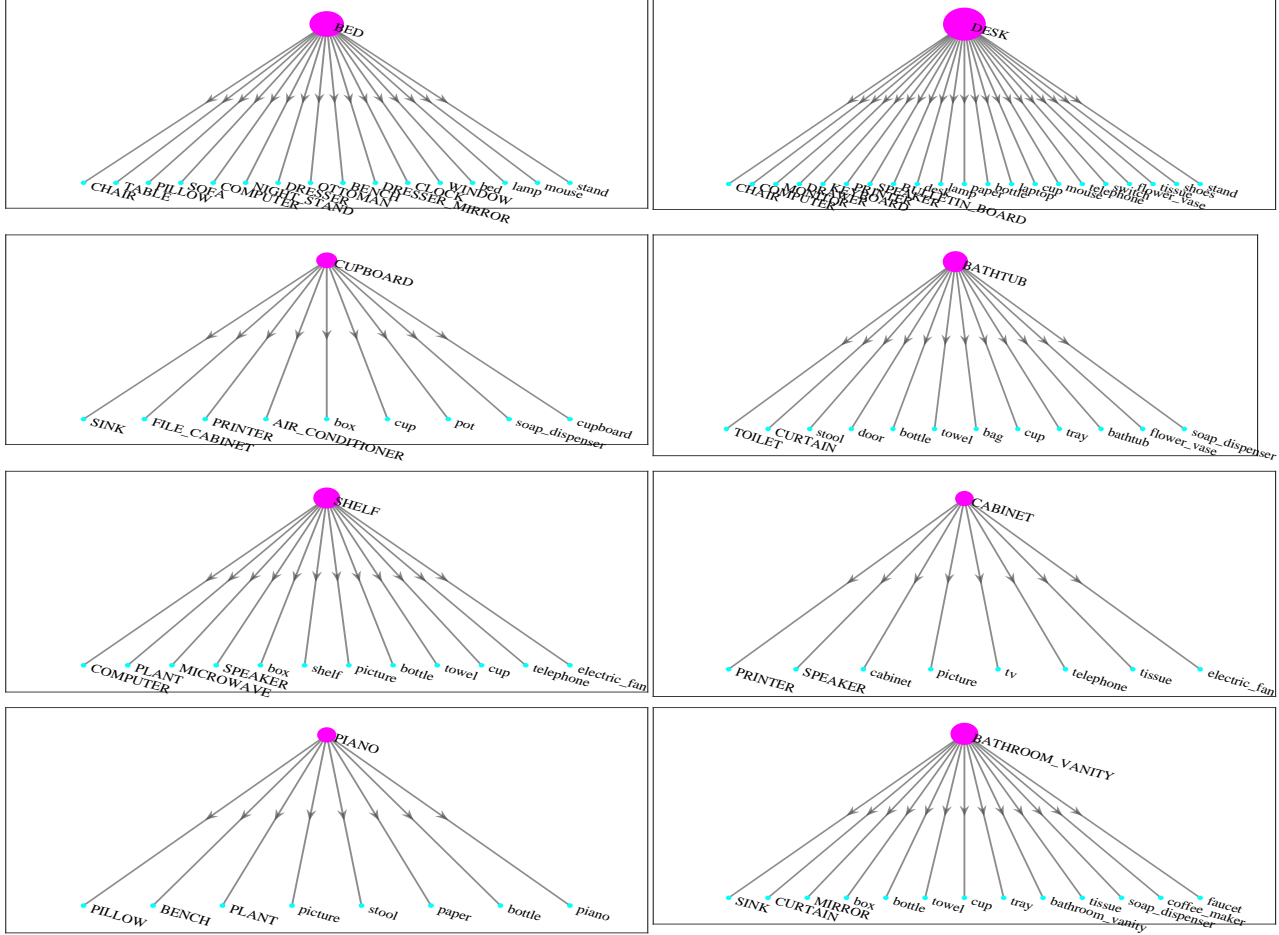


Figure 10. A few examples of the production rule-sets R_j which are utilized to generate the CFG. The detail algorithm is furnished in algorithm 3. The non-terminal symbols are displayed in upper-case and terminal symbols are shown in lower-case.

```

SHELF → None;
SCENE → piano PIANO SCENE;
PIANO → pillow PILLOW PIANO;
PIANO → bench BENCH PIANO;
PIANO → plant PLANT PIANO;
PIANO → picture PIANO;
PIANO → stool PIANO;
PIANO → paper PIANO;
PIANO → bottle PIANO;
PIANO → None;
SCENE → drawer DRAWER SCENE;
DRAWER → sink SINK DRAWER;
DRAWER → printer PRINTER DRAWER;
DRAWER → speaker SPEAKER DRAWER;
DRAWER → tv DRAWER;
DRAWER → bottle DRAWER;
DRAWER → tray DRAWER;
DRAWER → telephone DRAWER;
DRAWER → flower_vase DRAWER;
DRAWER → toilet_paper DRAWER;
DRAWER → electric_fan DRAWER;
DRAWER → coffee_maker DRAWER;
DRAWER → None;
SCENE → dresser DRESSER SCENE;
DRESSER → pillow PILLOW DRESSER;
DRESSER → night_stand NIGHT_STAND DRESSER;
DRESSER → box DRESSER;
DRESSER → lamp DRESSER;
DRESSER → tv DRESSER;
DRESSER → bottle DRESSER;
DRESSER → laptop DRESSER;
DRESSER → cup DRESSER;
DRESSER → None;
SCENE → sofa SOFA SCENE;
SOFA → pillow PILLOW SOFA;
SOFA → sofa_chair SOFA_CHAIR SOFA;
SOFA → endtable ENDTABLE SOFA;
SOFA → COFFEE_TABLE COFFEE_TABLE SOFA;
SOFA → cart CART SOFA;
SOFA → towel SOFA;
SCENE → night_stand NIGHT_STAND SCENE;
NIGHT_STAND → box NIGHT_STAND;
NIGHT_STAND → garbage_bin NIGHT_STAND;
NIGHT_STAND → lamp NIGHT_STAND;
NIGHT_STAND → bottle NIGHT_STAND;
NIGHT_STAND → telephone NIGHT_STAND;
NIGHT_STAND → None;
SCENE → BOOKSHELF BOOKSHELF SCENE;
BOOKSHELF → bulletin_board BULLETIN_BOARD BOOKSHELF;
BOOKSHELF → stool BOOKSHELF;
BOOKSHELF → paper BOOKSHELF;
BOOKSHELF → bottle BOOKSHELF;
BOOKSHELF → cup BOOKSHELF;
BOOKSHELF → None;
SCENE → COFFEE_TABLE COFFEE_TABLE SCENE;
COFFEE_TABLE → pillow PILLOW COFFEE_TABLE;
COFFEE_TABLE → sofa_chair SOFA_CHAIR COFFEE_TABLE;
COFFEE_TABLE → endtable ENDTABLE COFFEE_TABLE;
COFFEE_TABLE → paper COFFEE_TABLE;
COFFEE_TABLE → cup COFFEE_TABLE;
COFFEE_TABLE → tray COFFEE_TABLE;
COFFEE_TABLE → None;
SCENE → rack RACK SCENE;
RACK → printer PRINTER RACK;
RACK → towel RACK;
RACK → bag RACK;
RACK → None;
SCENE → dining_table DINING_TABLE SCENE;
DINING_TABLE → chair CHAIR DINING_TABLE;
DINING_TABLE → painting PAINTING DINING_TABLE;
DINING_TABLE → ottoman OTTOMAN DINING_TABLE;
DINING_TABLE → laptop DINING_TABLE;
DINING_TABLE → None;
SCENE → window WINDOW SCENE;
WINDOW → pillow PILLOW WINDOW;
WINDOW → plant PLANT WINDOW;
WINDOW → towel WINDOW;
WINDOW → None;
SCENE → endtable ENDTABLE SCENE;

```

```

ENDTABLE → microwave MICROWAVE ENDTABLE;
ENDTABLE → speaker SPEAKER ENDTABLE;
ENDTABLE → box ENDTABLE;
ENDTABLE → lamp ENDTABLE;
ENDTABLE → bottle ENDTABLE;
ENDTABLE → cup ENDTABLE;
ENDTABLE → tray ENDTABLE;
ENDTABLE → flower_vase ENDTABLE;
ENDTABLE → electric_fan ENDTABLE;
ENDTABLE → None;
SCENE → cabinet CABINET SCENE;
CABINET → printer PRINTER CABINET;
CABINET → speaker SPEAKER CABINET;
CABINET → picture CABINET;
CABINET → tv CABINET;
CABINET → telephone CABINET;
CABINET → tissue CABINET;
CABINET → electric_fan CABINET;
CABINET → None;
SCENE → dresser_mIRROR dresser_MIRROR SCENE;
dresser_MIRROR → tv dresser_MIRROR;
dresser_MIRROR → None;
SCENE → fridge FRIDGE SCENE;
FRIDGE → plant PLANT FRIDGE;
FRIDGE → microwave MICROWAVE FRIDGE;
FRIDGE → clock CLOCK FRIDGE;
FRIDGE → box FRIDGE;
FRIDGE → bottle FRIDGE;
FRIDGE → soap_dispenser FRIDGE;
FRIDGE → None;
SCENE → person PERSON SCENE;
PERSON → shoes PERSON;
PERSON → None;
SCENE → cart CART SCENE;
CART → keyboard KEYBOARD CART;
CART → printer PRINTER CART;
CART → bench BENCH CART;
CART → speaker SPEAKER CART;
CART → tv CART;
CART → mouse CART;
CART → None;
SCENE → file_cabinet FILE_CABINET SCENE;
FILE_CABINET → plant PLANT FILE_CABINET;
FILE_CABINET → microwave MICROWAVE FILE_CABINET;
FILE_CABINET → flower_vase FILE_CABINET;
FILE_CABINET → electric_fan FILE_CABINET;
FILE_CABINET → None;
SCENE → toilet TOILET SCENE;
TOILET → sink SINK TOILET;
TOILET → garbage_bin TOILET;
TOILET → paper TOILET;
TOILET → tissue TOILET;
TOILET → toilet_paper_dispenser TOILET;
TOILET → None;
SCENE → bulletin_board BULLETIN_BOARD SCENE;
BULLETIN_BOARD → clock CLOCK BULLETIN_BOARD;
BULLETIN_BOARD → laptop BULLETIN_BOARD;
BULLETIN_BOARD → ladder BULLETIN_BOARD;
BULLETIN_BOARD → None;
SCENE → bench BENCH SCENE;
BENCH → pillow PILLOW BENCH;
BENCH → podium BENCH;
BENCH → None;
SCENE → tv_stand TV_STAND SCENE;
TV_STAND → paper TV_STAND;
TV_STAND → tv TV_STAND;
TV_STAND → None;
SCENE → clock CLOCK SCENE;
CLOCK → pillow PILLOW CLOCK;
CLOCK → sofa_chair SOFA_CHAIR CLOCK;
CLOCK → ottoman OTTOMAN CLOCK;
CLOCK → switch CLOCK;
CLOCK → None;
SCENE → sink SINK SCENE;
SINK → microwave MICROWAVE SINK;
SINK → mirror MIRROR SINK;
SINK → bottle SINK;
SINK → towel SINK;
SINK → soap_dispenser SINK;
SINK → faucet SINK;
SINK → None;
SCENE → air_conditioner AIR_CONDITIONER SCENE;
AIR_CONDITIONER → curtain CURTAIN AIR_CONDITIONER;
AIR_CONDITIONER → ladder AIR_CONDITIONER;
AIR_CONDITIONER → None;
SCENE → sofa_chair SOFA_CHAIR SCENE;
SOFA_CHAIR → chair CHAIR SOFA_CHAIR;
SOFA_CHAIR → None;
SCENE → mirror MIRROR SCENE;
MIRROR → faucet MIRROR;
MIRROR → None;
SCENE → painting PAINTING SCENE;
PAINTING → switch PAINTING;
PAINTING → None;
SCENE → printer PRINTER SCENE;
PRINTER → tissue PRINTER;
PRINTER → None;
SCENE → plant PLANT SCENE;
PLANT → pot PLANT;
PLANT → electric_fan PLANT;
PLANT → None;
SCENE → curtain CURTAIN SCENE;
CURTAIN → garbage_bin CURTAIN;
CURTAIN → None;
SCENE → pillow PILLOW SCENE;
PILLOW → lamp PILLOW;
PILLOW → None;
SCENE → computer COMPUTER SCENE;
COMPUTER → keyboard KEYBOARD COMPUTER;
COMPUTER → mouse COMPUTER;
COMPUTER → None;
SCENE → whiteboard WHITEBOARD SCENE;
WHITEBOARD → picture WHITEBOARD;
WHITEBOARD → None;
SCENE → ottoman OTTOMAN SCENE;
OTTOMAN → cup OTTOMAN;
OTTOMAN → None;
SCENE → speaker SPEAKER SCENE;
SPEAKER → cup SPEAKER;
SPEAKER → None;
SCENE → monitor MONITOR SCENE;
MONITOR → keyboard KEYBOARD MONITOR;
MONITOR → None;
SCENE → chair CHAIR SCENE;
CHAIR → towel CHAIR;
CHAIR → None;
SCENE → keyboard KEYBOARD SCENE;
KEYBOARD → mouse KEYBOARD;
KEYBOARD → None;
SCENE → microwave MICROWAVE SCENE;
MICROWAVE → pot MICROWAVE;
MICROWAVE → None;
SCENE → None;

```

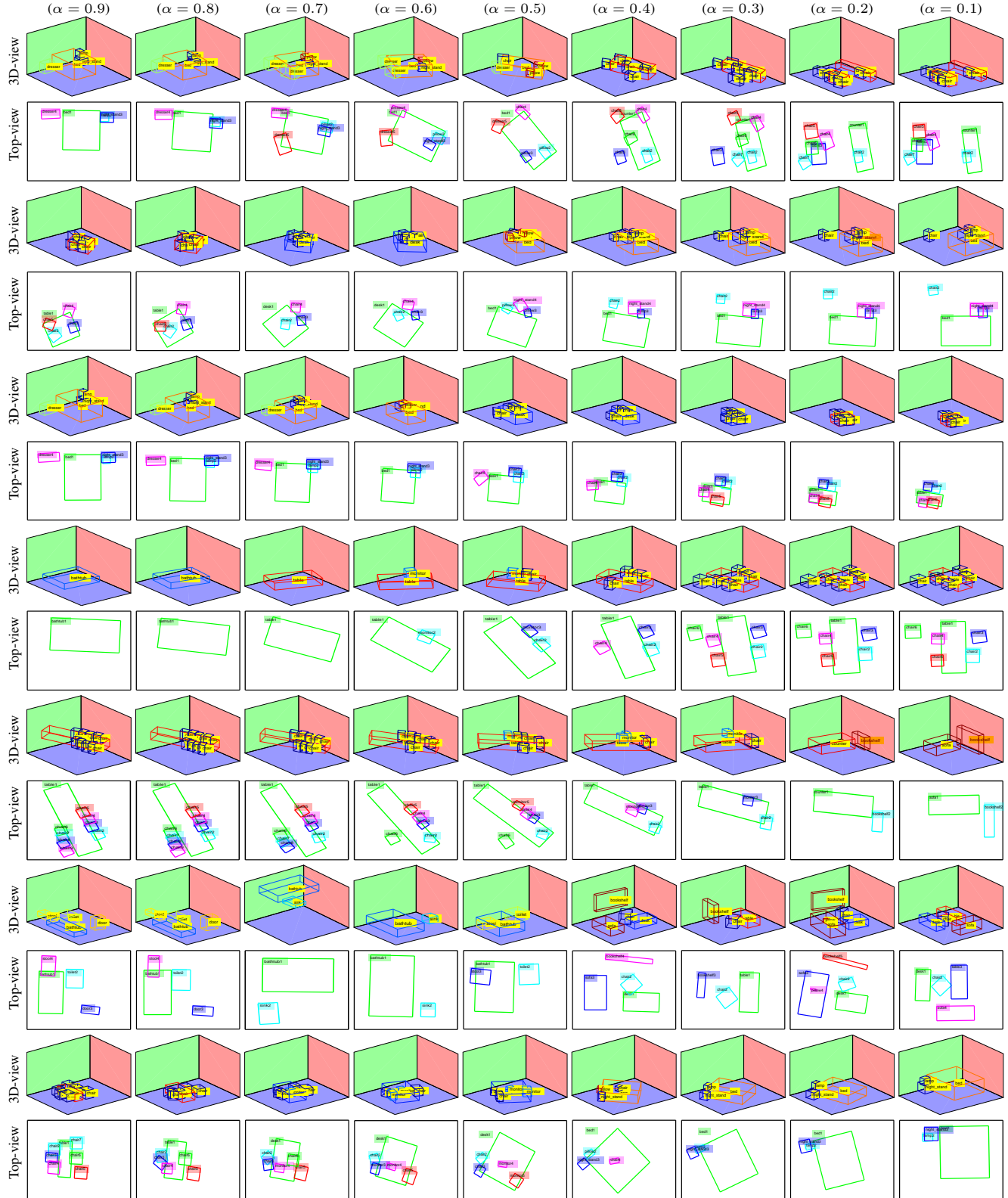


Figure 11. Synthetic scenes decoded from linear interpolations $\alpha\mu_1 + (1 - \alpha)\mu_2$ of the means μ_1 and μ_2 of the latent distributions of two separate scenes. The generated scenes are valid in terms of the co-occurrences of the object categories and their shapes and poses (more examples in the supplementary). The room-size and the camera view-point are fixed for better visualization. Best viewed electronically.

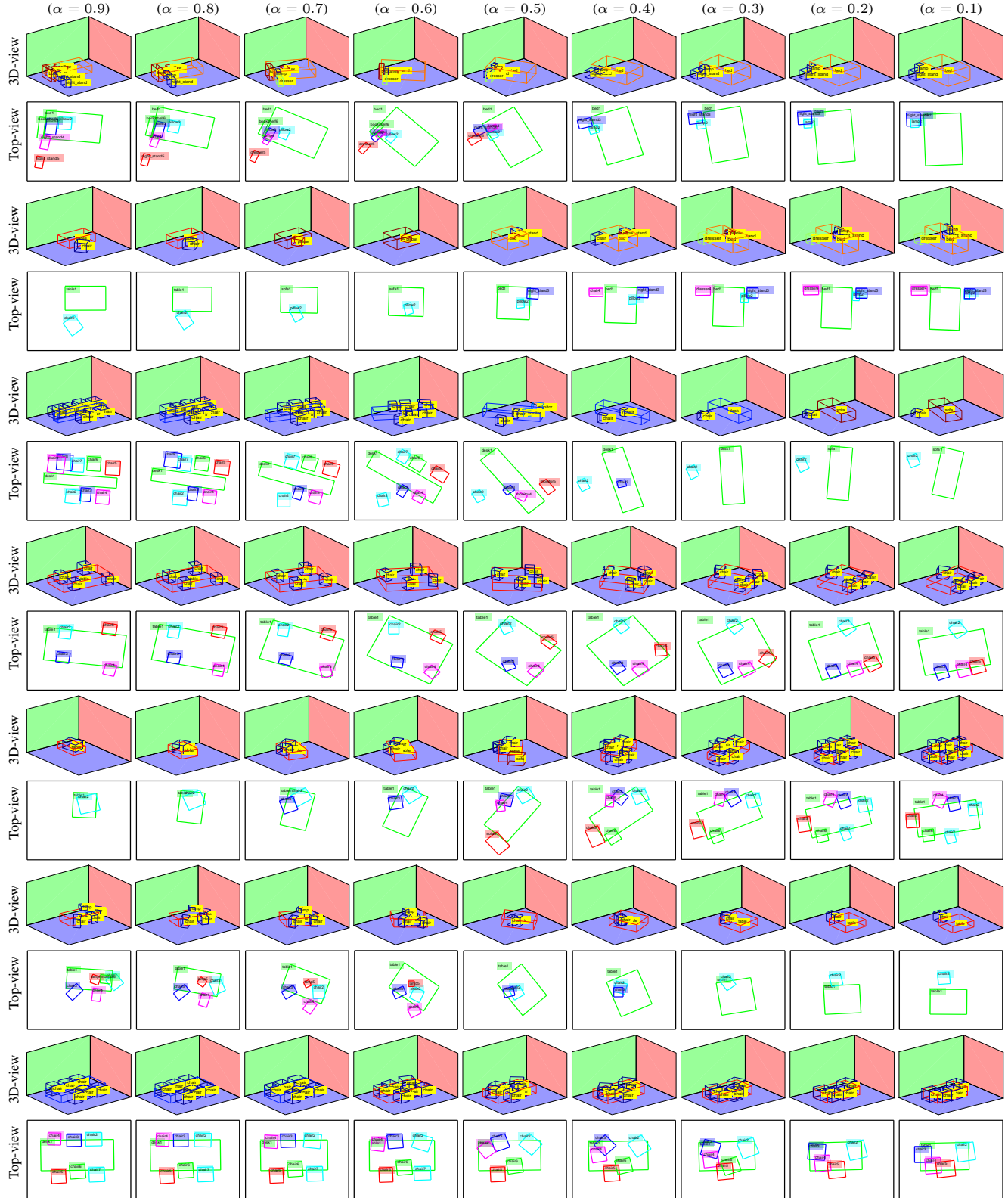


Figure 12. Synthetic scenes decoded from linear interpolations $\alpha\mu_1 + (1 - \alpha)\mu_2$ of the means μ_1 and μ_2 of the latent distributions of two separate scenes. The generated scenes are valid in terms of the co-occurrences of the object categories and their shapes and poses (more examples in the supplementary). The room-size and the camera view-point are fixed for better visualization. Best viewed electronically.

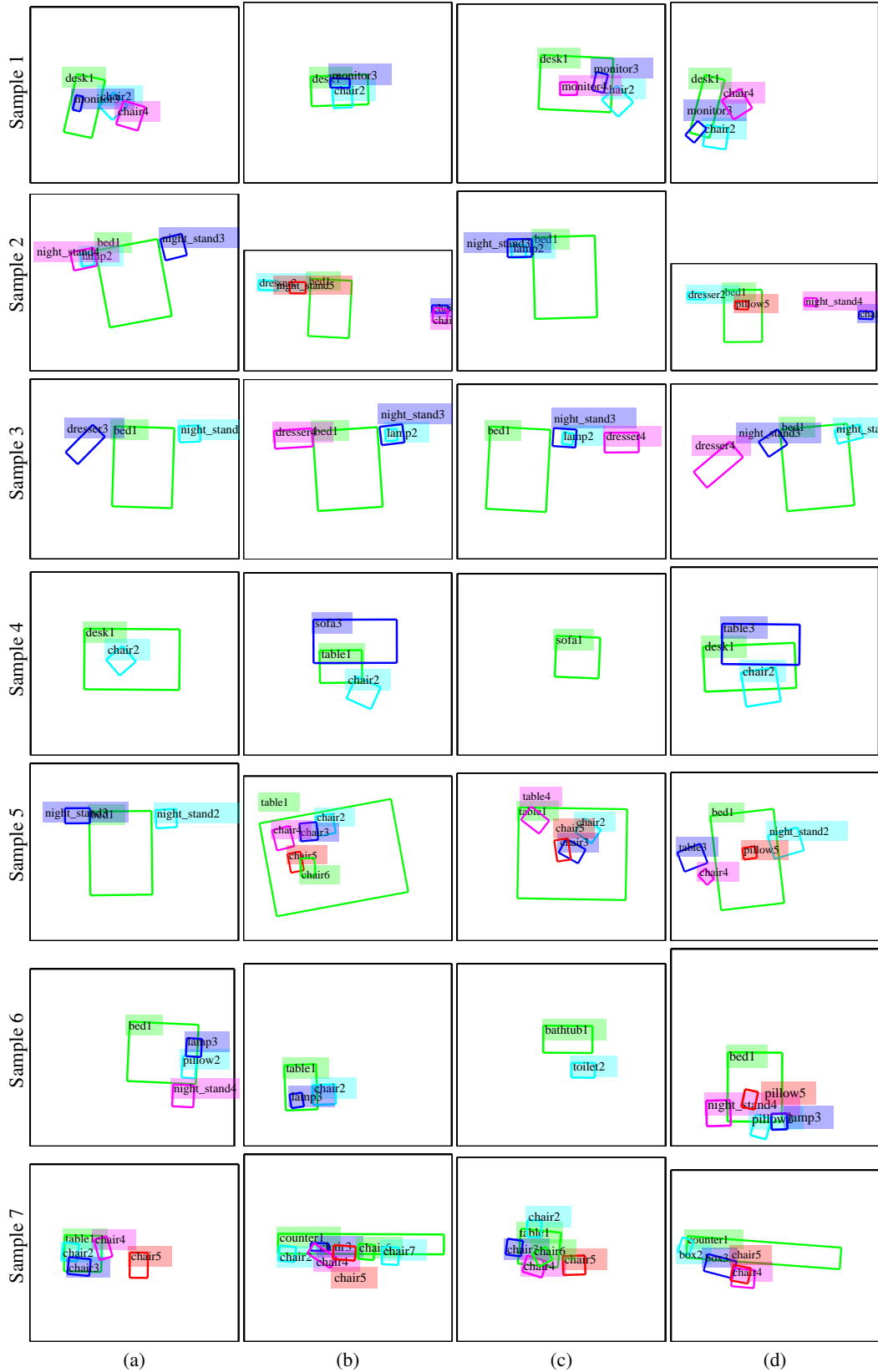


Figure 13. Arithmetic in latent space: latent vector of (d) is obtained by the sum of latent vectors of (a) & (b) and subtracted by (c), i.e. $(d) := (a) + (b) - (c)$. Note that in all the cases the synthesized scenes in (d) are meaningful in terms of arithmetic operations. In this figure, actual room size is displayed without changing the aspect ratios. In the other figures, a fixed aspect ratios are incorporated for visually pleasing display.

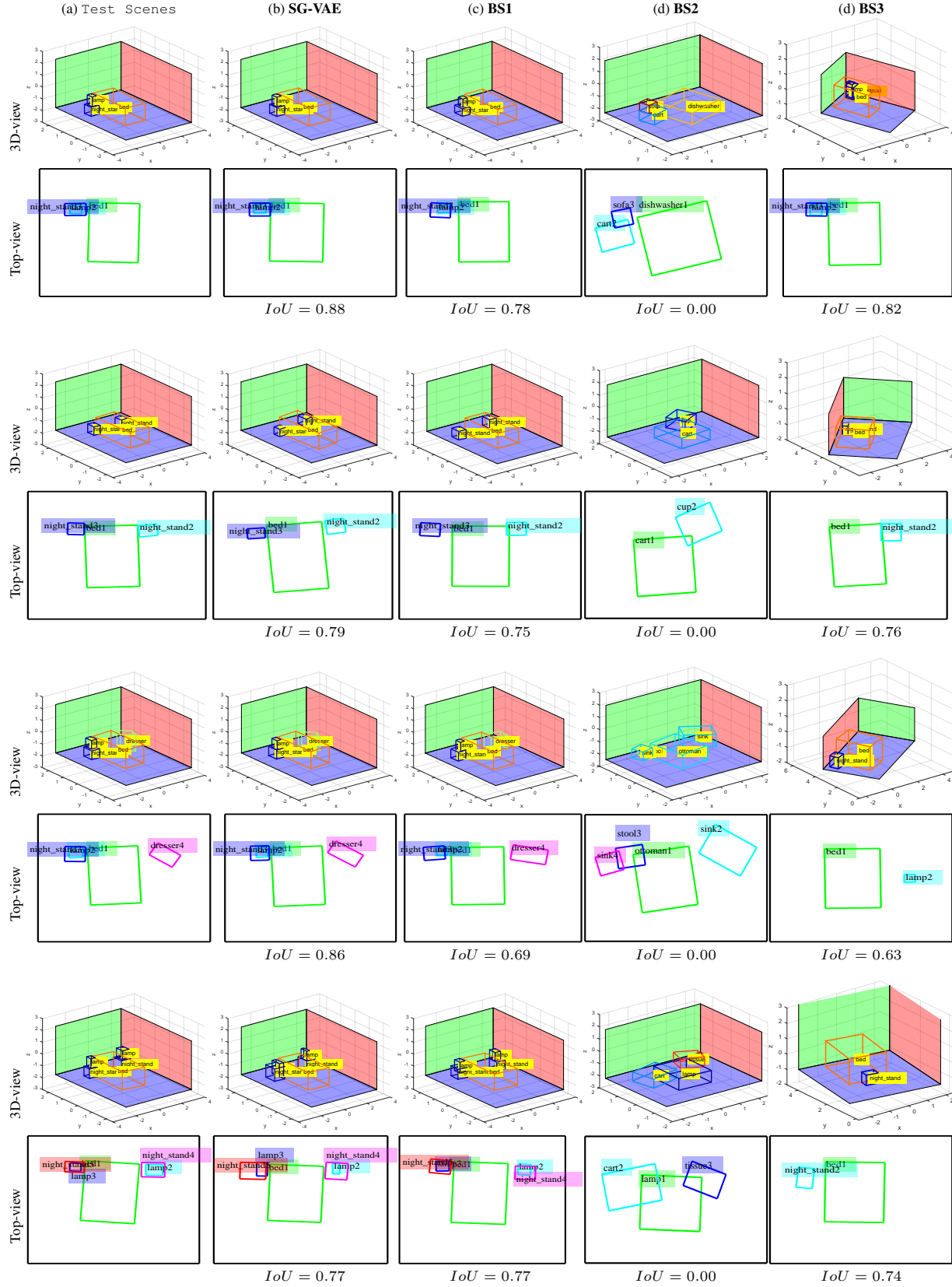


Figure 14. Qualitative results (reconstruction of the layouts) of the baseline auto-encoders on SUNRGB Datasets

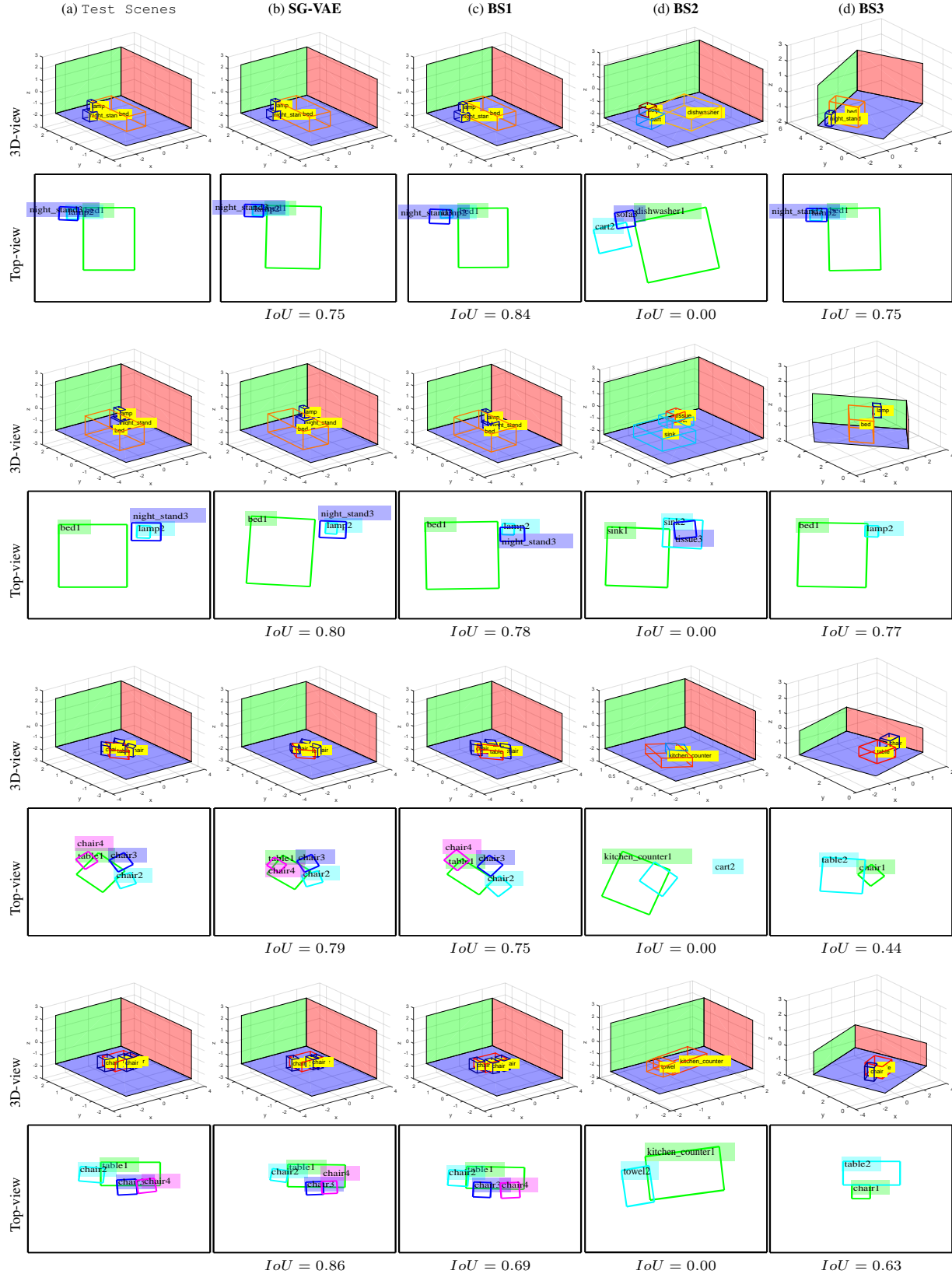


Figure 15. Qualitative results (reconstruction of the layouts) of the baseline auto-encoders on SUNRGBD Datasets